Recent Developments in the Chemistry and Physics of Metal Fullerides

M. J. Rosseinsky

Inorganic Chemistry Laboratory, Department of Chemistry, University of Oxford, South Parks Road, Oxford, United Kingdom OX1 3QR

Received April 1, 1998

The current status of metal intercalation into fullerene hosts is reviewed. The extent to which widely accepted simple models of the metallic and superconducting behavior in the A_3C_{60} compounds are sustainable is examined. The search for higher superconducting transition temperatures is discussed in the context of the synthesis of fullerides with different anion charges, more complex structures, and derived from higher fullerene hosts.

Contents

Introduction

Seven years have passed since the discoveries of conductivity[1] and superconductivity in alkali metal-intercalated C_{60}.[2] A wide variety of new solid-state science of particular relevance to intercalation chemistry, the physics of narrow-band systems, and the search for high superconducting transition temperatures in molecular conductors has been developed. It is now appropriate to consider whether there is anything more of interest that these materials can teach us. This review aims to cover recent developments in the field after a brief introduction to material covered in more detail in earlier review articles,[3−8] and is intended to complement the approaches of the recent reviews that focus on the effect of anion charge on physical properties[9] and on polymeric fullerides and heterofullerenes.[10] The influence of varying the anion charge on the electronic structure of metal fullerides, including the importance of chemical factors in controlling physical properties, is discussed in the first part of the article, and a review of recent work aimed at extending the scope of fulleride chemistry to structures other than simple sphere packings and hosts other than C_{60} is presented in the latter part of the article.

1. Background

The C_{60} molecule[11,12] has the well-known truncated icosahedron or "soccer ball" shape, with 60 equivalent carbon atoms arranged as 12 pentagons and 20 hexagons on the surface of a sphere of radius 3.56 Å. In the pure solid, *fcc* packing ($a = 14.17$ Å; $r(C_{60}-C_{60}) = 10$ Å) is adopted, with quasi-free molecular reorientation[13,14] replaced by orientational order in space group $Pa\bar{3}$ below 260 K.[15] The electronic structure of the molecule is important in determining the properties of the intercalates. The lowest unoccupied molecular orbital (LUMO) of C_{60} is almost nonbonding in nature, accounting for the electronegative character of the molecule, and is triply degenerate with t_{1u} symmetry. The t_{1g} "LUMO + 1" level is also chemically accessible, with possible anion charges of up to 12^- (Figure 1).

The extensive intercalation chemistry of *fcc* C_{60} derives from the weak inter-C_{60} forces and the well-documented size match between the octahedral and tetrahedral interstitial sites in the *fcc* C_{60} array and those of the cations of the electropositive elements.[8] The A_3C_{60} alkali metal fullerides are formed by complete occupancy of these sites. Cation ordering is observed when size differences are sufficiently pronounced (e.g., $Rb^T{}_2Cs^OC_{60}$, $Na^T{}_2Rb^OC_{60}$). The band derived from the t_{1u} orbital is half-filled at the 3^- anion charge, and, consistent with this, metallic behavior is observed experimentally.[1] The three-dimensionality of the *fcc* $C_{60}{}^{3-}$ array suppresses the low-dimensional metal−insulator transitions associated with previous classes of molecular conductors, and superconductivity[2] is observed at temperatures of up to 33 K in Cs_2RbC_{60} under ambient pressure.[16]

These high transition temperatures (T_c) have produced a very large body of work directed toward understanding the mechanism behind them and increasing them, resulting in a very strong experimental and theoretical focus on the A_3C_{60} composition. The BCS (Bardeen Cooper Schreiffer) theory, developed to account for superconductivity in metals and alloys with charge carriers in relatively broad bands, appears to account for many of the observations on these systems. In this model, superconductivity arises from the pairing

10.1021/cm980226p CCC: $15.00 Published 1998 by the American Chemical Society
Published on Web 10/02/1998

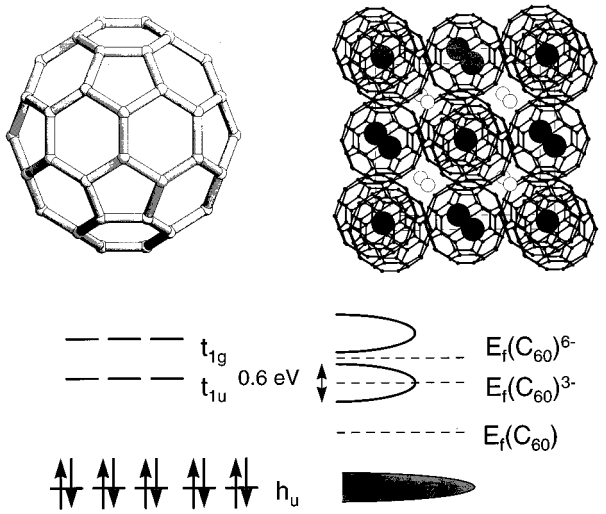

Figure 1. The HOMO, LUMO, and LUMO + 1 levels of the C_{60} molecule, and their evolution into narrow bands on the formation of the *fcc* solid. Dashed lines show the Fermi levels for neutral C_{60}, metallic K_3C_{60} and insulating K_6C_{60}. The structure of Rb_2CsC_{60} shows preferential occupancy of the octahedral site by the large Cs^+ cation (grey), with the smaller Rb^+ cation on the tetrahedral sites (white). The C_{60}^{3-} anions adopt the "standard" orientation as shown in Figure 3.

of electrons by their interaction with lattice vibrations, with the transition temperature being determined by the phonon frequency ω and the density of states at the Fermi level, $N(E_f)$, and the extent of coupling between the electrons and lattice vibrations, V. The weak-coupling BCS equation for T_c is

$$k_B T_c = \hbar\omega \exp\left(\frac{-1}{VN(E_f)}\right) \qquad (1)$$

Molecular conductors have long been considered good candidates for high T_cs because, in a simple-minded application of eq 1, the light atoms give high optic phonon frequencies and the poor intersite overlap (compared with metals and alloys) produces narrow bandwidths and high densities of states at the Fermi level. There are many experimental measurements on the A_3C_{60} superconductors that are consistent with a BCS model involving moderate ($\lambda \approx 0.5-1.0$) coupling to high-frequency vibrations of the C_{60}^{3-} anion, which has become widely accepted. There are problems with this approach, which will become clear during the course of this article. This has led to an intense theoretical debate concerning the applicability of the BCS model and its derivatives, all based on electron−phonon coupling, and to a search for experiments designed to unambiguously define the pairing mechanism.

The two key components of the BCS model are the involvement of phonons in the pairing (testable by the isotope effect on T_c and by the influence of electron−phonon coupling on the spectroscopic line widths of the vibrational modes) and the controlling influence of the density of states at the Fermi level. There is much evidence from neutron[17] and Raman[18,19] scattering for the existence of strong coupling between the t_{1u} electrons and H_g symmetry vibrations, but such coupling is expected on symmetry grounds alone and is not necessarily involved in producing pairing. The observed ^{13}C isotope effect[20,21] is in accord with BCS expectations

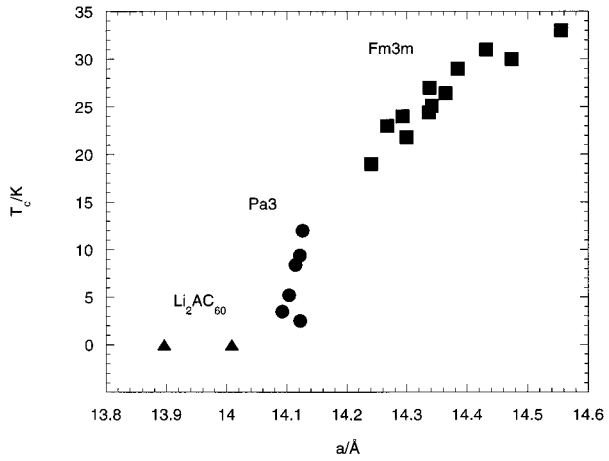

Figure 2. T_c as a function of lattice parameter in the cubic $A_{3-x}A'_xC_{60}$ phases. The enhanced variation of T_c with a in the $Pa\bar{3}$ family (circles) compared with the $Fm\bar{3}m$ family (squares), and the absence of superconductivity in the lithium fullerides (triangles) are noteworthy. Data for this figure are taken from refs 29, 39, 86, and 127.

but can be explained with zero-point modulation of the interfulleride transfer integral in an electronic pairing model.[22] Theories based on pairing mediated by other excitations, loosely characterized as electron−electron coupling, can make predictions hard to distinguish from those of BCS.[23] The essential feature of these models is minimization of the disruption to the π-bonding of C_{60} through correlation of the motion of the extra electrons in the t_{1u} orbitals: a detailed review is given by Gelfand.[6] Electron−electron interactions have been shown to be important in enhancing the normal state Pauli paramagnetic susceptibility[24−26] and determining the metallic resistivity, which is quadratic in T at low temperatures,[27] whereas the electron paramagnetic resonance (EPR) line width variation is consistent with electron−phonon coupling dominating conduction electron scattering.[28]

The BCS-like scaling of T_c with $N(E_f)$ is also a feature of electron−electron pairing models.[23] This prediction of eq 1 is in clear agreement with a wide variety of experimental work, building on initial correlations of T_c with *fcc* cell parameter (varied by modification of the mean A cation radius in an $A_2A'C_{60}$[29] series or by the application of hydrostatic pressure to a single A_3C_{60}[30,31]) and measurement of the density of states at the Fermi level in K_3C_{60} and Rb_3C_{60}.[24] Restricting consideration to chemically simple $A_{3-x}A'_xC_{60}$ compounds produces Figure 2, in which the simple BCS prediction of variation of T_c with a, and thus $N(E_f)$, appears to be directly confirmed. However, even in these alkali metal A_3C_{60} phases, the $T_c(a)$ curve becomes divided into a "large a" region and a "smaller a" region in which $T_c(a)$ tantalizingly assumes a much steeper gradient. The structures of the A_3C_{60} phases in each region differ, illustrating the extent to which fulleride electronic properties are controlled by the crystal structure.

The "large a" phases adopt the anion ordering first proposed by Stephens and co-workers[32] in space group $Fm\bar{3}m$. The large (in the sense that their radius is greater than the radius ratio estimate of the T site size for spherically disordered anions) tetrahedral site potassium cations orient the C_{60}^{3-} anions so that the hexagon centroids are directed along the ⟨111⟩ directions toward

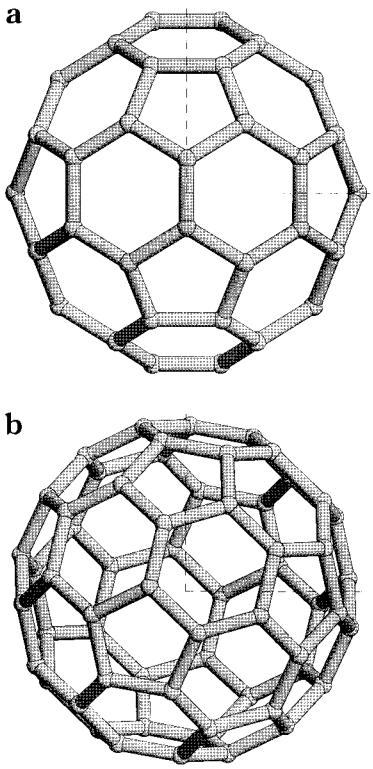

Figure 3. C_{60}^{3-} anion orientation in the $Fm\bar{3}m$ and $Pa\bar{3}$ A_3C_{60} structures, viewed along the cubic cell vectors. (a) $m\bar{3}$ symmetry standard orientation of the C_{60}^{3-} anion in K_3C_{60}. Two of these orientations, related by a 90° rotation about [001], are present in K_3C_{60}.[32] (b) $\bar{3}$ symmetry orientation found in the Na_2C_{60} and Na_2AC_{60} phases, and also in the low-temperature structure of C_{60} itself.[36−38,76] This orientation is produced by rotation of 22° away from the standard orientation about $\langle 111 \rangle$.

them. The C...K contacts thus favor an $m\bar{3}$ anion orientation in which the molecular mirror planes are aligned with the faces of the *fcc* unit cell (a so-called "standard" orientation). These orientations are long-range disordered to produce $Fm\bar{3}m$ symmetry with 50% occupancy of *each* standard orientation produced by 90° rotation about [001] (Figure 3a). The refined anion molecular structures conclusively indicate that the $Fm\bar{3}m$ symmetry arises from long-range disorder of locally well-defined anion orientations.[33] Calculations of the contribution of the t_{1u} bandwidth to the overall cohesive energy indicate that if both standard orientations are present, ordering in space group $P4_2/mnm$ is favored.[34] Neutron powder diffraction finds no long-range order of this type,[33] although radial distribution function measurements indicate that this ordering pattern may be locally favoured.[35] Figure 2 shows that, in this $Fm\bar{3}m$ family, T_c increases with a as expected from eq 1 if any changes in ω on expansion are dominated by the increase in $N(E_f)$ with decreasing overlap. Theoretical and experimental estimates of the precise values of $N(E_f)$ and their implications for the frequency of the pairing excitation and the extent of electron−electron interactions are continuing to provoke debate, as detailed in Section 2.1.

Changing the orientations of the fulleride anions exerts a striking influence on the $T_c(a)$ slope: the smaller Na^+ cation increases the relative importance of non-bonded C···C contributions to the cohesive energy[36] and produces the $Pa\bar{3}$ structure adopted by C_{60} in its orientationally ordered state below 260 K, in Na_2XC_{60} compounds, with lattice parameters of <14.17 Å.[37−39] The difference from the $m\bar{3}$ "standard" orientation is shown in Figure 3. The value of T_c increases much more rapidly with increasing a when the anions are oriented in this way than in the $Fm\bar{3}m$ structure. The fundamental reasons for this difference are still a matter of active debate because resolving these differences is essential to understanding how T_c is controlled by intermolecular overlap in the fulleride materials (Section 2.4).

At the opposite end of the $T_c(a)$ plot would lie a hypothetical Cs_3C_{60} *fcc* phase. This composition has been prepared by a low-temperature route and is stable at <180 °C.[40] However, Cs_3C_{60} is not isostructural with Cs_2RbC_{60} and the other *fcc* phases. It adopts the less dense, body-centered packing of the fulleride anions, being a mixture of a *bcc* phase (isostructural with Ba_3C_{60},[41] in which the Cs^+ cations are ordered in the so-called A15 structure) and a body-centered tetragonal phase in which the cation vacancies in the A_4C_{60} structure (Section 2.3.3) are disordered. The volume per C_{60}^{3-} anion is 815.3 and 830.9 Å^3 in the cubic and tetragonal phases, respectively, which is considerably expanded compared with the 770 Å^3 per anion in Cs_2RbC_{60}. Contrary to the *fcc* A_3C_{60} phases, T_c increases under pressure, attaining 40 K under 15 kbar, with a 25% volume fraction when corrected for the small particle size.[40] This unconventional pressure dependence is either attributable to granularity or to a difference in microscopic pairing mechanism from the *fcc* A_3C_{60} phases. The application of pressure appears to increase the quantity of the tetragonal phase. The search for expanded fullerides with a 3^- anion charge, to investigate whether T_c can be increased yet further, is therefore still an important task and an outstanding issue in the area.

2. Current Issues in the A_3C_{60} Phases

At first sight, the metallic behavior in the formally half-filled band and the simple relationship between T_c and A_3C_{60} lattice parameter are readily explicable by the conventional band and BCS theories already outlined, suggesting that further study of these systems is superfluous. But detailed examination of a range of experimental data and parameter values in theoretical models reveals several problems with this explanation. The resolution of these issues will determine the extent to which the behavior of electrons in narrow bands derived from degenerate basis orbitals is understood. The A_3C_{60} phases thus continue to pose important questions, addressed in this section.

From a chemical viewpoint, the absence of a satisfactory, predictive theory of T_c, exemplified by the unconventional behavior of Cs_3C_{60}, provides a continuing motivation to explore the synthesis of new fullerides, an important test of theories of pairing in the "high T_c" region being the preparation a range of expanded systems with more complex structures than the simple *fcc* and *bcc* structures studied thus far. Following this section, the article focuses on the synthesis of new fulleride structure types (in Sections 3 and 4), and the exploration of the physical properties of fullerides with charges other than 3^-, including higher fullerides (in Sections 5−7).

2.1. Interelectron Repulsion, Bandwidth, and Electronic Structure in the A_3C_{60} Metals. A prerequisite for the simple models discussed in the Background Section and widely accepted as correct for the metal fullerides is that the half-filled band in C_{60}^{3-} gives rise to metallic behavior. This assumption depends on the electronic kinetic energy, defined by the t_{1u} bandwidth W, being the dominant energy scale. The weak interaction between t_{1u} wave functions on neighboring C_{60} molecules requires that the basis for this assumption is tested critically. As detailed by Gunnarsson,[5] the situation in the A_3C_{60} phases is in fact complex, with intramolecular phonon frequencies and, of particular importance for this section, interelectron repulsion energies being comparable to W.

The onsite interelectron repulsion U (defined as the difference between the ionization energy and the electron affinity) acts to oppose the tendency of the electrons to delocalize and reduce their kinetic energy by introducing an energy penalty for double occupancy of a given site. This phenomenon is very important in solid-state science and gives rise to the idea of a Mott−Hubbard insulator, in which a partially filled band does not produce a metal.[42] For the free C_{60} molecule, experiment shows $2.7 \leq U/\text{eV} \leq 3.0$, compared with a theoretical estimate of 3.0 eV.[5] In the solid, U is always reduced from this gas-phase value due to the polarization of surrounding molecules upon the charge separation (eq 2), which U describes:

$$2C_{60}^{3-} \rightarrow C_{60}^{2-} + C_{60}^{4-} \qquad (2)$$

This reduction results in theoretical estimates of this parameter in the solid of $0.8 \leq U/\text{eV} \leq 1.3$.[43] The first measurement, from Auger spectroscopy in neutral C_{60}, yielded $U = 1.6 \pm 0.2$ eV.[44] A subsequent measurement yielded $U = 1.4$ eV in K_3C_{60} itself.[45] Diminished screening at the surface is estimated to require reduction of these values by 0.3 eV to give U in the bulk solid.[46]

Direct experimental measurement of the bandwidth W in K_3C_{60} is difficult because of the simultaneous excitation of plasmons and phonons on photoionization: a review of photoelectron spectroscopy (PES) estimates is given by Weaver and Poirier.[47] Local density approximation (LDA) band-structure calculations are generally thought reliable in this regard, although the $Fm\bar{3}m$ A_3C_{60} structures, with long-range disorder of the two standard orientations, produce rather severe problems for this approach.[48] The important general conclusion is that, regardless of which theoretical approach or model for the observed disorder is used, no estimate of W approaches the size of U. Band structure calculations indicate a significant alteration of the electronic structure between the $Fm\bar{3}$ (ordered anions, one orientation; the closest experimental realization of this is the C_{60}^{5-} phase Ba_2CsC_{60}[49]) and $P4_2/mnm$ (ordered, two standard orientations) structures, with the 0.52 eV bandwidth in $Fm\bar{3}$ increasing to 0.64 eV in the bidirectional structure due to the better overlap between t_{1u} orbitals on C_{60} neighbors with opposite standard orientations.[50] These bandwidths are predicted to decrease by ∼15% upon expansion to Rb_3C_{60}, which leads to estimates of the ratio U/W of between 1.25 and 2.6 for K_3C_{60}, and larger values for the more expanded Rb_3C_{60} and $RbCs_2C_{60}$. Current understanding of the single-band Hubbard model gives the critical U/W ratio to produce insulating behavior as between 1 and 1.5,[51] placing stoichiometric K_3C_{60} into the Mott−Hubbard insulator category. Therefore the observed metallic behavior must be due either to inadequacies in this theory as applied to fullerides or to an incomplete understanding of key experimental facts. One interpretation is that the observed metallic behavior near half-filling is due to *deviations* from the K_3C_{60} composition, with the physics being that of a doped Mott insulator.[44] In view of the importance of the Mott−Hubbard model in understanding high T_c superconductors (now widely considered as doped Mott−Hubbard insulators) and doped compensated semiconductors, the A_3C_{60} compounds have turned out to be significant test cases for this theory. This has stimulated detailed experimental measurements to answer difficult questions concerning the precise structure and composition of materials available only as air-sensitive powders. In view of the estimates of U/W, if the simple theories outlined in the Background Section do actually work, it is important to know why.

The key difference between the actual electronic structure of the fullerides and existing theoretical models is the degeneracy of the t_{1u} orbitals. The advent of the U/W question in the fullerides has stimulated theoretical work on the Mott−Hubbard model applied to orbitally degenerate systems. Advances in theory call into question the conclusion based on single-band Mott−Hubbard models that the range of current estimates for U and W necessarily mean that stoichiometric K_3C_{60} would be an insulator. Recent work indicates that the critical U/W ratio for electron localization is crucially influenced by the orbital degeneracy N at each site.[43,52] This influence occurs because the availability of extra orbital states opens hopping channels that are unavailable in the absence of degeneracy, allowing the extra electron in the charge-disproportionated state in eq 2 to hop in one of three ways to each neighboring site without any extra repulsion energy, if singlet nearest neighbor correlations predominate (Figure 4(a)). This reduces the gap from $U-W$ to $U-\sqrt{N}W$, and increases the critical ratio to $(U/W)_c \sim 2.5$,[43] which places the transition beyond the range of experimentally observed U/W. Metallic stoichiometric A_3C_{60} is now theoretically reconcilable with the experimentally observed U and theoretical estimates of W. The metallic state with U significantly greater than W is unusual and would be strongly correlated; theoretical predictions indicate the Pauli susceptibility should be enhanced by a factor of between two and three from that expected solely from the bandwidth.[53]

The considerations just presented take C_{60} to be a "superatom" with little regard to its internal electronic structure. In fact there are intramolecular electronic energy scales that are also comparable to U and W, and complicate the applicability of simple theoretical models to the fullerides (Figure 4(b)). The interelectron repulsion produces "on-ball" multiplet splitting of the $(t_{1u})^3$ configuration into the Hund's rule ^4A ground state and the Jahn−Teller unstable doublets ^2H and ^2T. Estimates of the exchange integral K give a total multiplet splitting of ∼0.15 eV,[53] which is comparable with the Fermi energy in K_3C_{60}. The orbital degeneracy of the

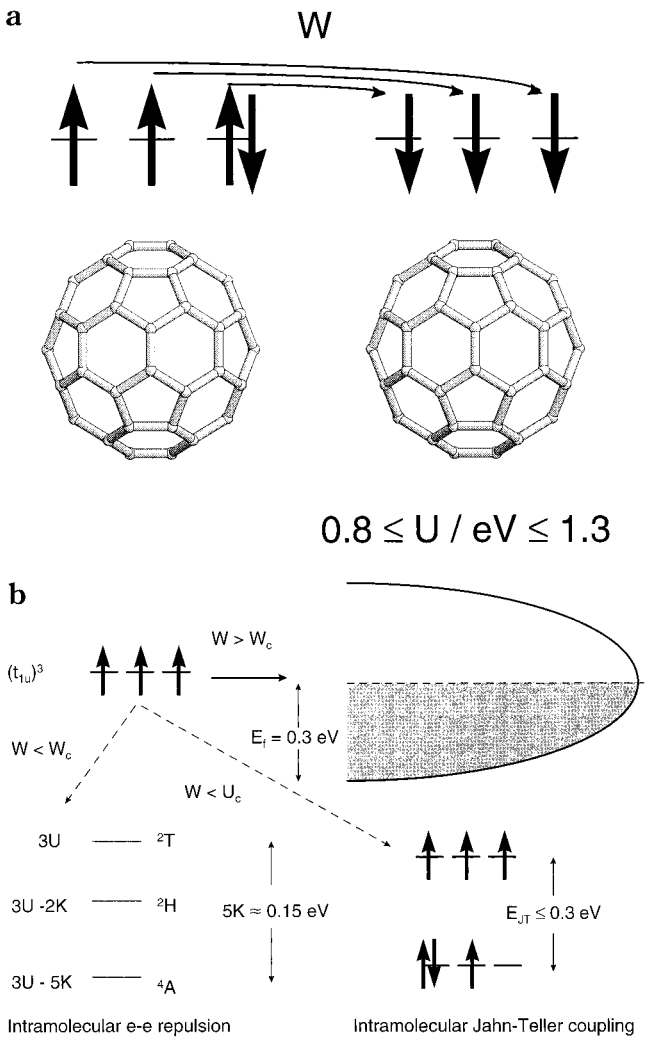

Figure 4. (a) The bandwidth W is favored over the interelectron repulsion U in orbitally degenerate systems due to the availability of more than one channel for hopping between neighboring fulleride anions, as illustrated qualitatively in the large U limit here.[43,52] The bandwidth depends sensitively on the type of anion orientational order, as discussed in the text. The kinetic energy of the extra electron in the t_{1u} level, formed by the charge fluctuation in eq 2, is reduced in an orbitally degenerate system, thereby decreasing the Mott−Hubbard gap. (b) Competing energies in solids containing the C_{60}^{3-} anion. If the bandwidth W is larger than a critical value W_c, defined by the size of U, the electrons become delocalized in a narrow band. The ground state of the localized C_{60}^{3-} anion is determined by the competition between the multiplet splitting energy (favoring a high-spin anion ground state[53,56]) and the on-ball Jahn−Teller energy, favoring the doublet states.[54] These intramolecular energies are important, even for the metallic state, because of the low Fermi energy.

doublet states allows Jahn−Teller distortion by coupling to the H_g vibrational modes, which are also implicated in the popular model for the superconductivity. Models incorporating electron−phonon coupling only indicate that the doublet states are lowest in energy, with a Jahn−Teller stabilization of up to 0.3 eV, and predict a "negative U" favorable Jahn−Teller contribution to the disproportionation in eq 2.[54] In the solid, the extent of this Jahn−Teller coupling will be controlled by the competition between this energy and the bandwidth. These competing energies, plus configuration interaction with the nearby t_{1g} levels, create ambiguity in theoretical prediction of the ground state of the C_{60}^{3-} anion.

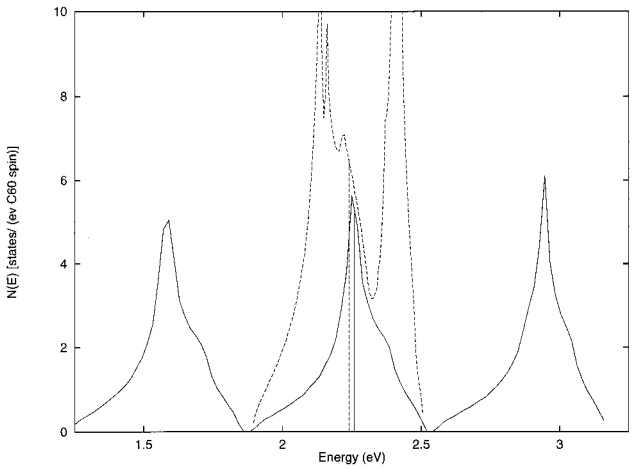

Figure 5. Calculated density of states for the t_{1u} LUMO band in an $Fm\bar{3}$ symmetry A_3C_{60} phase using equal orbital population (dashed line) or disproportionation among the components of the t_{1u} level in an orbitally polarized manner.[57] The Fermi level in each case is indicated by a vertical line. (Reproduced by permission from ref 57).

These calculations are for the isolated molecule, where careful experimental measurements by Reed and coworkers indicate that the doublet ground states are also favored in isolated anion salts,[55] with the caveat that the observed magnetism is quite consistent and with many states having energies comparable with the ground state for both the C_{60}^{2-} and C_{60}^{3-} anions. The most recent DFT calculations, allowing for Jahn−Teller anion geometry relaxation in the orbitally degenerate terms, indicate that the Hund's rule ground state ^4A is indeed lowest in energy but separated by only 0.03 eV from the Jahn−Teller distorted doublet.[56] The electron−phonon and multiplet interactions are of similar size but stabilize different states; the success of simple band theory, which is rather unexpected given consideration of the competing energies, may arise from an offsetting of these two factors.

The size of interactions between electrons occupying different t_{1u} orbitals on the C_{60}^{3-} anion and its comparability to the bandwidth produces the unusual situation in which the metallic state could contain a high degree of orbital polarization. A recent calculation explicitly taking into account differences in interelectron repulsion between electrons occupying the components of the t_{1u} manifold singly or doubly predicts just such an unequal orbital occupancy,[57] splitting the initially cubic band into three distinct subbands to optimize both interelectron repulsion and Jahn−Teller stabilization energy (Figure 5). This procedure produces both a steep decrease in $N(E_f)$ when the t_{1u} band is not half-full and a reduction in the sensitivity of the bandwidth to orientational order. These features may be important in the light of the experimental data summarized in Section 2.3. The calculated value of $N(E_f)$ is 6 states/(eV spin C_{60}) at half-filling, with a bandwidth of 1.05 ± 0.15 eV.

2.2. Composition and Structure of A_3C_{60}. The demonstration that U was comparable with, indeed larger than, W in the fullerides seemed incompatible with the observed metallic behavior, leading to suggestions that deviations from the ideal A_3C_{60} composition were present, making the t_{1u} band less than half-full and allowing the holes introduced by this "self-doping"

to carry charge. If the "A_3C_{60}" compounds have to be nonstoichiometric to be metallic, the basic physical picture underlying the superconductivity changes drastically. Several experiments addressing the structure and composition of A_3C_{60} have been performed. Detailed analyses of synchrotron X-ray powder diffraction data[58,59] indicate less than complete occupancy of the tetrahedral site, corresponding to refined compositions $Rb_{2.93(3)}C_{60}$ and $K_{2.91(2)}C_{60}$. The observation of a third resonance in the ^{87}Rb NMR of Rb_3C_{60} (the so-called T′ signal, seen in addition to the expected octahedral and tetrahedral (T) signals)[60] which is associated, and in dynamic equilibrium, with the majority T resonance from the tetrahedral site has been used as further evidence for these tetrahedral vacancies. The T:T′ intensity ratio of 11:2 can be explained if the T′ resonance arises from the six T sites neighboring an Rb vacancy on the tetrahedral site if the vacancy concentration is 0.06.[61] However, recent ^{87}Rb spin−echo double resonance (SEDOR) measurements indicate that this T,T′ splitting, seen also in site-ordered Rb_2CsC_{60}, does not arise from the presence of vacancies,[62] leaving only X-ray powder diffraction as the experimental evidence for deviation from the A_3C_{60} composition. These vacancies may not, however, now be required to explain the metallic and superconducting behavior. The absence of a connection between the T′ signal and any metal vacancies does however have disquieting implications for the current understanding of the local structure of A_3C_{60} compounds, because the T′ ^{87}Rb NMR resonance is now unexplained. Detailed neutron[33] and X-ray[59] powder diffraction studies of K_3C_{60} and Rb_3C_{60}, respectively, find no evidence for anion orientations other than $m\bar{3}$, which might otherwise produce different tetrahedral environments, and do not indicate any static displacement of the octahedral cation away from the site center.

2.3. Charge Dependence of the Electronic Properties. It now appears that the applicability of simple band theory concepts to the A_3C_{60} compounds results from the operation of an unexpected set of circumstances, namely the influence of the t_{1u} orbital degeneracy and the offsetting influences of the intramolecular multiplet and electron−phonon coupling energies. Changing the occupancy of the t_{1u} orbitals will clearly change the relative importance of these competing energies against the bandwidth. The properties of fullerides with anion charges other than 3 are therefore important to understand to judge the influence of these factors on fulleride ground states. Recent work indicates that anion charge is extremely significant in altering both the normal state and superconducting properties of fullerides.

2.3.1. Superconductivity and Anion Charge in Nearly Half-Filled t_{1u} Bands. Figure 6 shows the striking effect of variation of the anion charge around 3^- in the $Na_2Cs_xC_{60}$ ($0 \le x \le 1$) and $K_{3-x}Ba_xC_{60}$ ($0 \le x \le 0.4$) phases.[63] The superconducting transition temperature is a sharply peaked function of the anion charge, maximized at 3^-, and with a narrow superconducting composition range before nonsuperconducting behavior occurs at the integral anion 4^- and 5^- charges. The implications of this work are described in detail in a recent review,[9] but the important conclusion is worth

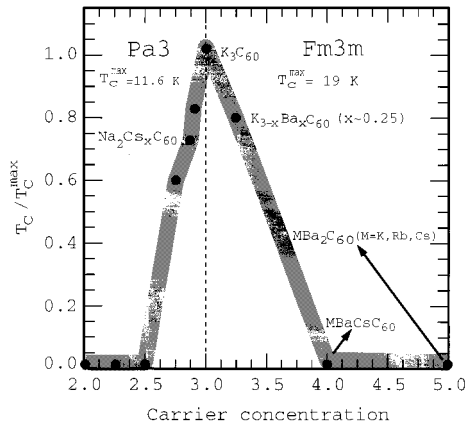

Figure 6. Plot of T_c/T_c^{max} versus carrier concentration, n, in the t_{1u} band for A_3C_{60} compounds. T_c is scaled using the T_c for the end members Na_2CsC_{60} and K_3C_{60}. The heavy line connecting the points is a guide for the eye and indicates upper bounds on the uncertainties in T_c and n. Note the narrow range of superconducting compositions and the sharp variation of T_c around half-filling. Reproduced by permission from ref 63.

restating here: this observation requires very sharp variation in $N(E_f)$ around half-filling of the t_{1u} band in BCS-like theories and is in sharp disagreement with those electron−electron pairing schemes placing emphasis on odd versus even electron counts. The orbitally polarized band structure presented in ref 57 does yield such a sharply peaked $N(E_f)$ function (Figure 5). The tendency for the experimentally observed merohedral disorder to broaden sharp features in $N(E)$ has been noted.[64] There are some extra experimental subtleties; they are, the structure of Ba_2CsC_{60} differs from that of K_3C_{60} in terms of anion orientational order,[49] and the $Na_2Cs_xC_{60}$ system is not isostructural with $K_{3-x}Ba_xC_{60}$, but this striking valence dependence of T_c must be theoretically explained before any understanding of the fulleride superconductors can be claimed.

2.3.2. Structure and Properties of fcc A_3C_{60} as the Anion Charge Varies. Large deviation from the 3^- charge within the *fcc* structure produces the nonsuperconducting $MBaCsC_{60}$ (4^-) and Ba_2AC_{60} (5^-) phases.[49,63] The synthesis of these *fcc* 4^- and 5^- A_3C_{60} phases in principle allows a more direct comparison with A_3C_{60} *fcc* C_{60}^{3-} systems than is possible with the *bct* A_4C_{60} phases discussed in Section 2.3.3. The absence of superconductivity above 2 K for both electron counts is hard to account for either with conventional band theory ($N(E_f)$ should be similar according to calculation, although the measured Pauli susceptibility $N_\chi = 1$ state eV^{-1} $spin^{-1}$ C_{60}^{-1} [63] is much lower than that of K_3C_{60}), or using electronically driven pairing. Most calculations show, however, that the electronic structure depends sensitively on the extent of orientational order. This result may be significant in these alkaline-earth-containing materials because neutron powder diffraction and ^{133}Cs NMR show surprising differences in detail from the $Fm\bar{3}m$ A_3C_{60} systems. Ba_2CsC_{60}, prepared by liquid ammonia reduction of C_{60}, is not strictly isostructural with the alkali metal compounds. Nine percent of the cesium cations occupy the tetrahedral sites, and the anions predominantly (83%) adopt one of the two possible standard orientations, producing a more ordered (space group $Fm\bar{3}$) A_3C_{60} with only 17%, rather than 50%, orientational defects (Figure 7).[49] Band

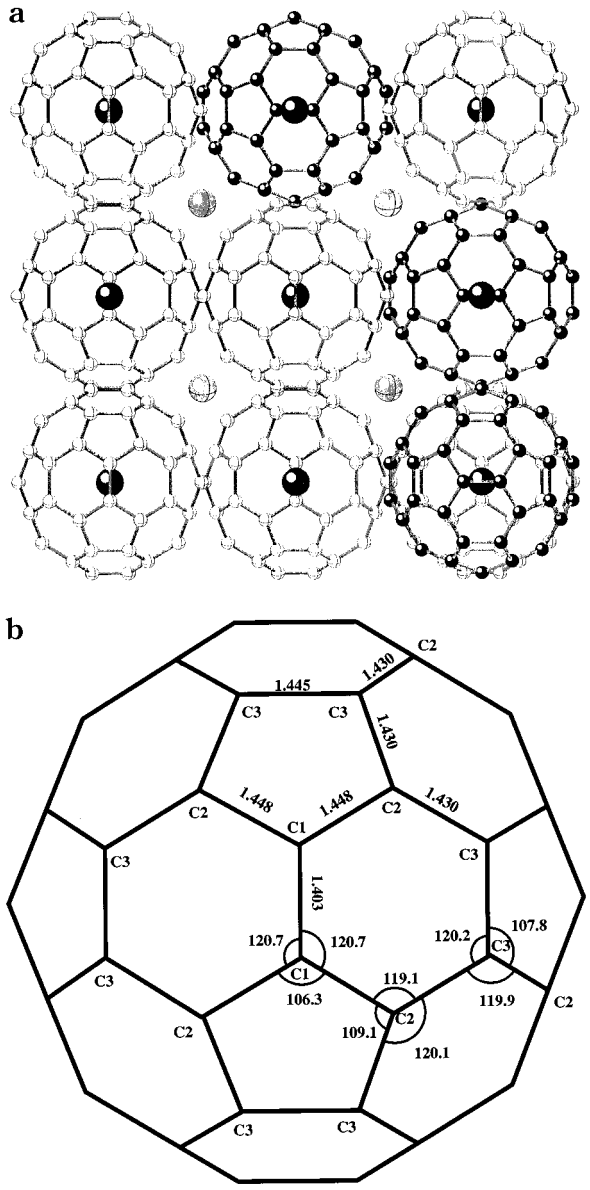

Figure 7. (a) The $Fm\bar{3}$ structure of Ba_2CsC_{60}; 83% of the anions (light gray) adopt one of the two standard orientations. The ^{133}Cs NMR results show that the octahedral site (dark gray spheres) is 91% occupied by cesium cations. (b) Bond lengths and angles in the C_{60}^{5-} anion in Ba_2CsC_{60}. Reproduced by permission from ref 49.

structure calculations (Section 2.1) indicate a significant alteration of the electronic structure between the $Fm\bar{3}$ and $P4_2/mnm$ structures.[50] The $N(E_f)$ for a C_{60}^{5-} phase with these structures is calculated to be comparable with that of K_3C_{60}, indicating that a non-band-structure explanation for the reduced Pauli susceptibility is required. The refined geometry of the C_{60}^{5-} anion is consistent with those of the C_{60}^{3-} and C_{60}^{6-} species, with the loss of distinction between 6:6 "double" and 6:5 "single" bonds being intermediate between that found for the two other charges (Figure 7(b)).[33]

2.3.3. Body-Centered Tetragonal A_4C_{60} Phases—Band, Mott−Hubbard, or Jahn−Teller Insulators? The quite different behavior at the 4^- anion charge seen in the *fcc* alkali metal/alkaline earth fullerides was preceded by the absence of superconductivity in the body-centered tetragonal ("*bct*") A_4C_{60} (A = K, Rb, Cs) phases. These compounds have a body-centered array of C_{60}^{4-} anions

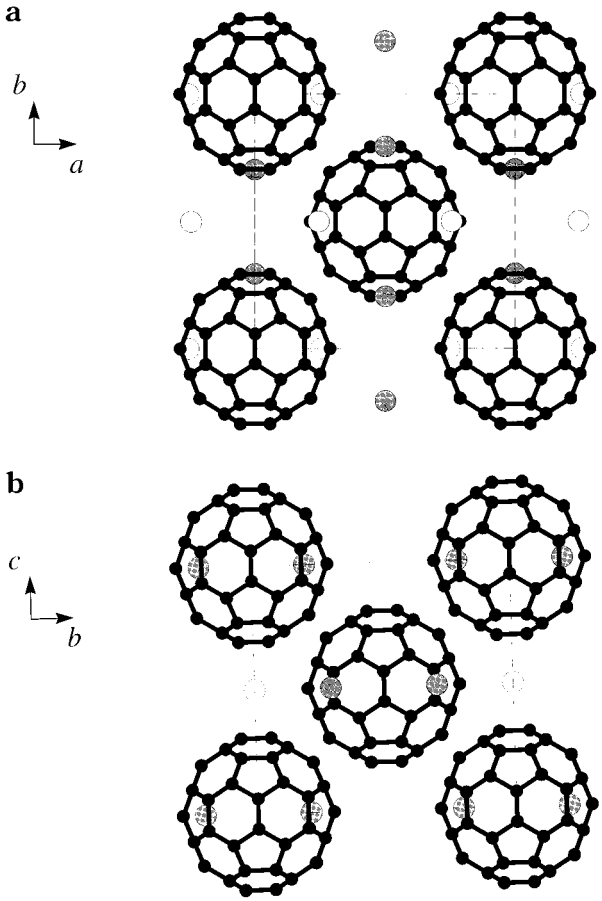

Figure 8. The orientationally ordered *Immm* structure of Cs_4C_{60}. There are two distinct Cs cation sites, shown as unshaded and light gray.[74] (a) view along the [001] axis, showing the orientational ordering of the C_{60}^{4-} anions with the 6:6 bond along the orthorhombic *b*-axis; (b) the ordering of the cation vacancies is shown in the *bc* plane.

in which 2/3 of the distorted tetrahedral sites in K_6C_{60} are occupied in an ordered manner[65] (Figure 8). These A_4C_{60} phases are attracting an increasing amount of theoretical and experimental attention in an effort to account for the absence of metallic behavior despite the 2/3 filling of the t_{1u} band. Band structure calculations[66] give a bandwidth (0.56 eV) comparable to that of K_3C_{60}. In contrast to A_3C_{60}, the even number of electrons per primitive unit cell in principle allows a "band structure" explanation of the insulating behavior, involving splitting the t_{1u} orbitals to produce two lower filled bands and one upper empty band. However, calculations indicate that the tetragonal component of the crystal field is insufficiently effective in lifting the t_{1u} degeneracy to explain the nonmetallic behavior[67−70] at ambient pressure. Alternative explanations of the insulating behavior at the C_{60}^{4-} charge have recently come to light, indicating the influence of both electron−electron and electron−phonon interactions. Clear candidates are the operation of the Mott−Hubbard mechanism, already discussed in detail for the C_{60}^{3-} charge, and lifting of the $(t_{1u})^4$ orbital degeneracy by Jahn−Teller distortion of the anion to form a singlet ground state that necessarily gives rise to an insulating solid. The role of anion orientational disorder is also unclear.

A recent electron energy loss spectroscopy (EELS) study compared the optical conductivity of the *bct* A_4C_{60}

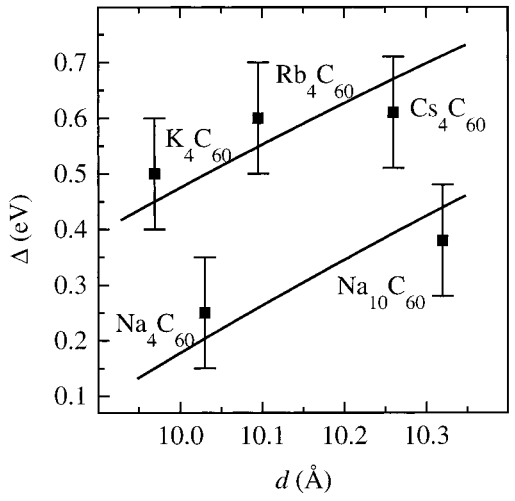

Figure 9. Energy gap determined by EELS for *bct* and *fcc* A_4C_{60} and *fcc* $Na_{10}C_{60}$. The lines indicate the expected variation in the Mott−Hubbard gap for *fcc* (lower) and *bct* (upper) phases. Reproduced with permission from ref 71.

phases (A = K, Rb, Cs) with an *fcc* Na_4C_{60} phase and $Na_{10}C_{60}$, taken to have a C_{60}^{8-} configuration[71] (Figure 9). The scaling of the optical gap with interfulleride spacing indicated that it corresponded to a transition between the lower and upper Hubbard subbands, with the differences between the two structural classes being consistent with models for the Mott−Hubbard gap in the orbitally degenerate fullerides already discussed.[43] This explanation is in contrast with interpretations based on the Jahn−Teller effect in the $(t_{1u})^4$ configuration, where degeneracy lifting on distortion produces the band gap: this explanation was ruled out due to the dependence of the observed gap on interfulleride separation. The derived gaps are rather larger than excitation energies identified by NMR and magnetic probes,[68,69] which were interpreted in terms of Jahn−Teller splittings of the order of 0.1 eV. The EELS study also indicates Jahn−Teller distortion of the molecule through the splitting of the $t_{1u}-t_{1g}$ transition.

Precise powder X-ray refinements indicate that K_4C_{60} and Rb_4C_{60} are line phases with compositions corresponding within error to an integral number of electrons per anion, in contrast to the previous work on the A_3C_{60} system.[72] This integral occupancy is consistent with the suggestion of a Mott−Hubbard gap for the C_{60}^{4-} phases.

Cs_4C_{60} has until recently not been reported as a pure phase, perhaps due to slow Cs^+ cation diffusion. The $I4/mmm$ structure of the *bct* K_4C_{60} and Rb_4C_{60} phases[65] is due to merohedral disorder over two equivalent orientations[72,73] (rotated by 45° from those in K_3C_{60}), as the point symmetry of $4/mmm$ is incompatible with subgroups of I_h. Increasing the cation size to Cs^+ suppresses the orientational disorder and produces an orthorhombic distortion to $Immm$ point symmetry (Figure 8) because the optimal Cs...pentagon and Cs...hexagon distances are sufficiently different to produce two different cesium cation sites and orientationally order the C_{60}^{4-} anions.[74] The mmm point symmetry of the C_{60}^{4-} anion in Cs_4C_{60} will totally lift the t_{1u} degeneracy, and thus the orientational ordering pattern is consistent with a Jahn−Teller distortion. The EELS data show this orientationally ordered phase to be insulating like its *bct* counterparts, demonstrating that the insulating nature of the *bct* A_4C_{60} compounds is not due to anion orientational disorder. The imposition of orientational order by Cs^+ in body-centered fulleride arrays also has consequences for the detailed structures of both Cs_3C_{60} phases in the 40 K superconductor.[40] This orthorhombic orientationally ordered structure has recently been observed for the Sr_4C_{60} and Ba_4C_{60} alkaline earth superconductors.[75]

The behavior of the "*bct*" C_{60}^{4-} salts is thus consistent with the combined importance of electron−electron and electron−phonon interactions. Recent evidence is in favor of a Mott−Hubbard rather than Jahn−Teller origin for the gap (the predicted Jahn−Teller stabilization energies of 0.2−0.3 eV are insufficient to overcome the calculated bandwidth). The singlet ground state of the C_{60}^{4-} anion[68] in these phases, however, indicates that the t_{1u} degeneracy must be lifted sufficiently to violate Hund's rules. This indication is consistent with the orientational order observed in Cs_4C_{60}. A unifying picture for the A_4C_{60} systems is that the on-site repulsion U localizes the t_{1u} electrons, which then produce the Jahn−Teller distortion. The synergic operation of electron−electron and electron−phonon coupling appears to produce an unusual Mott−Hubbard insulating ground state in which there are no local magnetic moments. This is in clear contrast to the well-studied magnetic Mott−Hubbard insulators found in, for example, many first row transition metal oxides such as La_2CuO_4. The behavior of the A_4C_{60} compounds indicates the extent to which electron−electron and electron−phonon interactions, not readily apparent from experiment in the A_3C_{60} case due to the metallic behavior, are generally operative in the fullerides. Viewed as a relative of A_4C_{60} reached by oxidation, the A_3C_{60} compounds do appear to be doped Mott−Hubbard insulators, regardless of their precise composition.

2.4. Orientational Order, Universal $T_c(a)$ Behavior, and Polymerization in Na_2AC_{60} Phases. The observation of low superconducting transition temperatures, a distinct orientational ordering[37,38] ($Pa\bar{3}$) from that of K_3C_{60} and a steep variation of T_c with a[39] have resulted in continued interest in the behavior of the site-ordered $Na^T{}_2A^OC_{60}$ phases.[76] An early suggestion to account for the distinct behavior was that $N(E_f)$ was a more sharply varying function of interfulleride separation in the $Pa\bar{3}$ phases. This issue has been addressed in wide-ranging studies of the dependence of $N(E_f)$ on orientation state and interfulleride separation. The ^{13}C NMR Knight shift (proportional to $N(E_f)$ in simple models) is linearly related to the lattice parameter in *all* cubic A_3C_{60} phases (Figure 10), showing that $N(E_f)$ is independent of the orientational order of the anions. Application of the McMillan equation (a generalization of eq 1 to account for the competing influence of electron−electron repulsion[77]) using the deduced densities of states to calculate T_c yields a weighted phonon frequency of 600 K.[78] The controlling influence of center-to-center fulleride separation rather than anion orientation on $N(E_f)$ was confirmed in EPR measurements[79] of the normal state susceptibility, which find a much sharper universal experimental dependence of $N(E_f)$ on interfulleride separation (defined as $d = \{(a/\sqrt{2}) - 7.04\}$Å), which is again independent of $Pa\bar{3}$ or $Fm\bar{3}m$ orientational order. The deduced

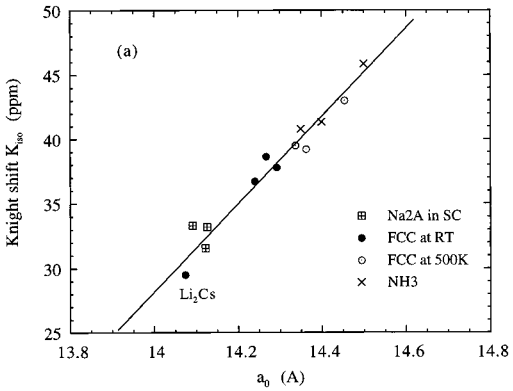

Figure 10. The correlation between ^{13}C NMR Knight shift and cubic lattice constant for $Fm\bar{3}m$ and $Pa\bar{3}$ phases with a C_{60}^{3-} charge, including the $(NH_3)NaA_2C_{60}$ systems with cation disorder on the octahedral site. Reproduced with permission from ref 78.

functional form for the bare susceptibility (appropriate for comparison with band structure values), using thermal expansion to model the temperature dependence of the unenhanced susceptibility, is exponential, which is in agreement with theoretical estimates[50] and given in eq 3 ($\alpha = 3 \times 10^{-4}$, $\beta = 0.25$).

$$N(E_f) = \left(\frac{\alpha}{d}\right) \exp\left(\frac{d}{\beta}\right) \quad (3)$$

The derived Stoner enhancement of the bare susceptibility is half that previously deduced.[24,25] This result is consistent with the observed $T_c(a)$ relationship, and quantitative analysis yields a low phonon frequency (180 K) with a very small interelectron repulsion parameter, μ^*, of 0.01.

There is thus no obvious explanation in terms of normal-state electronic properties for the pronounced difference in superconducting behavior between the $Fm\bar{3}m$ and $Pa\bar{3}$ families. Recent diffraction[80] and NMR[81] work reveals that a polymeric ground state is in competition with the cubic metallic superconductors in C_{60}^{3-} systems below a critical interfulleride separation corresponding to Na_2CsC_{60} (the point where the $Fm\bar{3}m$ and $Pa\bar{3}$ $T_c(a)$ curves meet). The close $C_{60}-C_{60}$ contacts in Na_2RbC_{60} produce a transition from the $Pa\bar{3}$ structure to a nonsuperconducting polymer below 230 K; the superconducting cubic phase can be quenched to low temperature, reconciling early disagreements over whether Na_2RbC_{60} and Na_2KC_{60} were actually superconducting.[76,82] The structure of the polymer itself is important as it clearly demonstrates the anion charge state will determine the preferred polymerization route. One-dimensional polymer chains are formed by single C−C bond formation between neighboring C_{60}^{3-} anions, which is in marked contrast to the formation of two bonds by [2+2] cycloaddition in neutral C_{60} and C_{60}^{1-} polymers due to the availability of sufficient t_{1u} electrons at the C_{60}^{3-} anion charge to form a chain of interfulleride single bonds (Figure 11). The cubic $Pa\bar{3}$ structure is stable at all temperatures for Na_2CsC_{60}, which is above the critical interfulleride separation for polymerization to occur. The suppressed T_c with respect to the $Fm\bar{3}m$ phases as the interfulleride distance contracts may be related to this tendency to polymerize rather than to orientational control of any of the

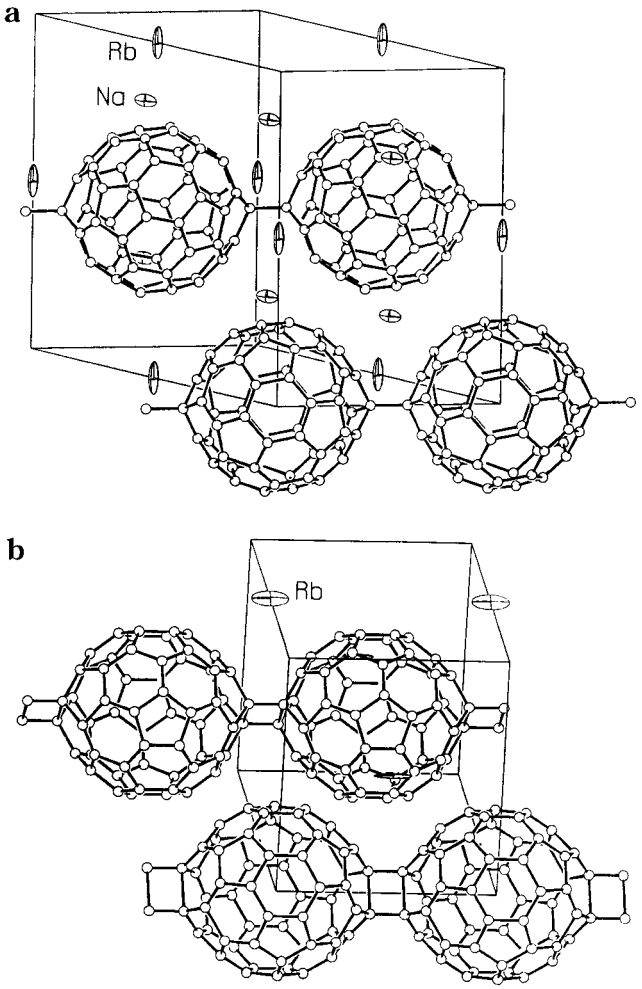

Figure 11. (a) Crystal structure of the polymeric form of Na_2RbC_{60}, which is stable on slow cooling below 230 K. One-dimensional polymer chains are formed by single bonds between C_{60}^{3-} monomer units. The structure contrasts with the [2+2] polymer shown in (b),[128] where two single bonds bridge each monomer unit. Reproduced with permission from ref 80.

parameters in the BCS/McMillan equation. The influence of this radical anion polymerization chemistry on the physics of superconductivity is clearly of interest for future investigation.

One accepted feature of the model for fulleride superconductivity is that the alkali metal cations influence T_c only to second order, so the application of pressure to Rb_3C_{60} will give the same T_c as found for an $A_2A'C_{60}$ mixed-metal fulleride.[30,31] Recent precise determination of the pressure dependence of structure and transition temperature in Rb_3C_{60} indicates the alkali cations can actually exert significant effects, with a much *less* pronounced reduction of T_c on application of pressure than is produced by cation substitution[83] (Figure 12). This absence of universality even in the $Fm\bar{3}m$ regime requires modification of theories that only treat the lattice parameter as important, regardless of the chemical composition. The absence of any ^{87}Rb isotope effect does, however, conclusively rule out pairing via low-frequency $M^+ - C_{60}^{3-}$ vibrations.[84] Details such as the evolution of the T′ NMR resonance on cation substitution and the influence of cation site disorder on T_c in the $A_{3-x}A'_xC_{60}$ phases now need to be addressed; substitutional disorder at the electronically inactive

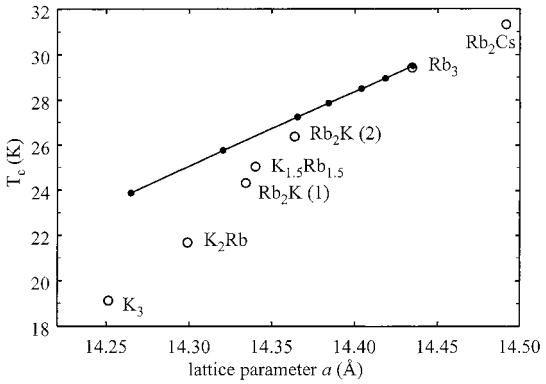

Figure 12. Plot of T_c versus 298 K lattice parameter for Rb_3C_{60} (filled circles), connected by a solid line as a guide to the eye. The open circles correspond to $Fm\bar{3}m$ $A_{3-x}A_xC_{60}$ phases.[29] A difference between the effect of hydrostatic pressure and that of chemical pressure shown in Figure 2 is clearly apparent, breaking the universal T_c versus a correlation. Reproduced with permission from ref 83.

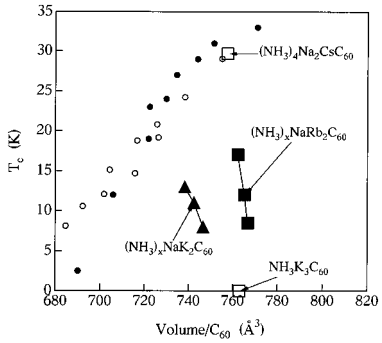

Figure 13. Variation of T_c with unit cell volume for ammoniated fullerides with linear $Na-NH_3$ complexes (filled squares and triangles) occupying the octahedral site. The inversion of the $T_c(V)$ relation that holds in the A_3C_{60} phases with octahedral site species compatible with cubic symmetry (spherical A^+ or tetrahedral $(NH_3)_4Na^+$)) is clear. Reproduced with permission from ref 87.

perovskite A cation site has recently been shown to play a significant role in controlling the properties of colossal magnetoresistive manganese oxides.[85]

3. Ammoniated A_3C_{60} Fullerides—New Perspectives on Fulleride Structure and Electronic Properties

3.1. Superconducting and Insulating Ground States in $(NH_3)_xA_3C_{60}$ Phases. The elemental cations considered thus far are spherical and thus produce rather simple, high-symmetry fulleride structures related to the familiar *fcc* and *bcc* sphere packings. Molecular or complex counterions offer the opportunity to obtain quite different packing motifs by exploiting more directional or specific anion−cation interactions. Complexation of the metal cations in a fulleride array can produce simple isotropic expansion (e.g., reaction of Na_2CsC_{60} with ammonia yields $[(NH_3)_4Na]^ONa^TCs^TC_{60}$[86]), which lies on the universal ambient pressure $T_c(a)$ curve found for the $Fm\bar{3}m$ A_3C_{60} superconductors (Figure 13). However, the potential mismatch between the symmetry of the anion packing and the complex cation geometry offers an opportunity to create local disorder or produce a significant distortion from cubic symmetry. The first set of solids we consider involves the low-temperature formation of a linear $[NH_3-M]^+$ complex cation on the octahedral site in the presence of an *fcc* packing of fulleride anions.

The $(NH_3)_xNaA_2C_{60}$ ($x \approx 1$ A = K, Rb) phases[87,88] are prepared by direct reaction of the metals in liquid ammonia with C_{60} followed by low-temperature vacuum deammoniation. These compositions do not form in the absence of the ammonia ligand. The compounds are *fcc* with a linear $Na-NH_3$ unit on the octahedral site displaced by 0.4−0.6 Å from the site center, the Na−N bond being disordered over the eight equivalent ⟨111⟩ directions. The lattice parameter a is varied by controlling the NH_3 content via the final deammoniation temperature. These heavily cation-disordered phases retain superconductivity, as expected for strictly cubic C_{60}^{3-} compounds, but the variation of T_c with a is strikingly different from that observed in the previously studied $Fm\bar{3}m$ phases, where the species on the octahedral site have spherical or tetrahedral symmetry compatible with that of the anion packing (Figure 13). The T_c value is *much lower* than would be expected from the lattice parameter according to the universal curve, and strongly decreases with increasing a in each family. The association between the suppression of T_c and the inversion of the influence of a on T_c with the strong static disorder on the octahedral site is very striking. It is particularly important in the context of the superconducting pairing mechanism that the ^{13}C Knight shift, and thus the density of states at the Fermi level, is exactly what would be expected from the *fcc* lattice parameter (Figure 10). The disorder is thus not directly responsible for a sharp reduction in the value of $N(E_f)$ below that expected from the observed interfulleride separation. The application of weak-coupling BCS to these systems appears doubtful, unless clear evidence for radically altered phonon frequencies or electron−phonon coupling can be found.

Cation displacement from the octahedral site center was first demonstrated in $(NH_3)K_3C_{60}$, again due to the formation of a linear $M-NH_3$ unit.[89] In this case, the larger complex cation produces a tetragonal distortion of the *fcc* unit cell, with the expansion in volume per C_{60}^{3-} anion occurring together with displacement of four of the initial 12 neighbors of a C_{60}^{3-} anion to 10.52 Å away, retaining eight 10 Å contacts in an anion environment intermediate between *bcc* and *fcc* (Figure 14). The original X-ray Rietveld refinement was unable to distinguish statistically between orientationally disordered $Fmmm$ and orientationally ordered $I4/mmm$ space groups, the orthorhombic structure being preferred due to more physical K...C contacts. Neutron powder diffraction is required to unambiguously determine the anion orientation.

$(NH_3)K_3C_{60}$ is of importance in demonstrating the influence of symmetry on both the normal and superconducting states in C_{60}^{3-} systems. Although the volume per C_{60}^{3-} anion is close to that found for Rb_3C_{60} and slightly smaller than in the largest member of the cubic, but disordered $(NH_3)_xNaRb_2C_{60}$ family, the anisotropic distortion of the fulleride packing produces a suppression of superconductivity. The temperature-independence of the EPR-derived magnetic susceptibility and the ^{13}C Knight shift indicate that the distorted C_{60}^{3-} array does retain metallic conductivity how-

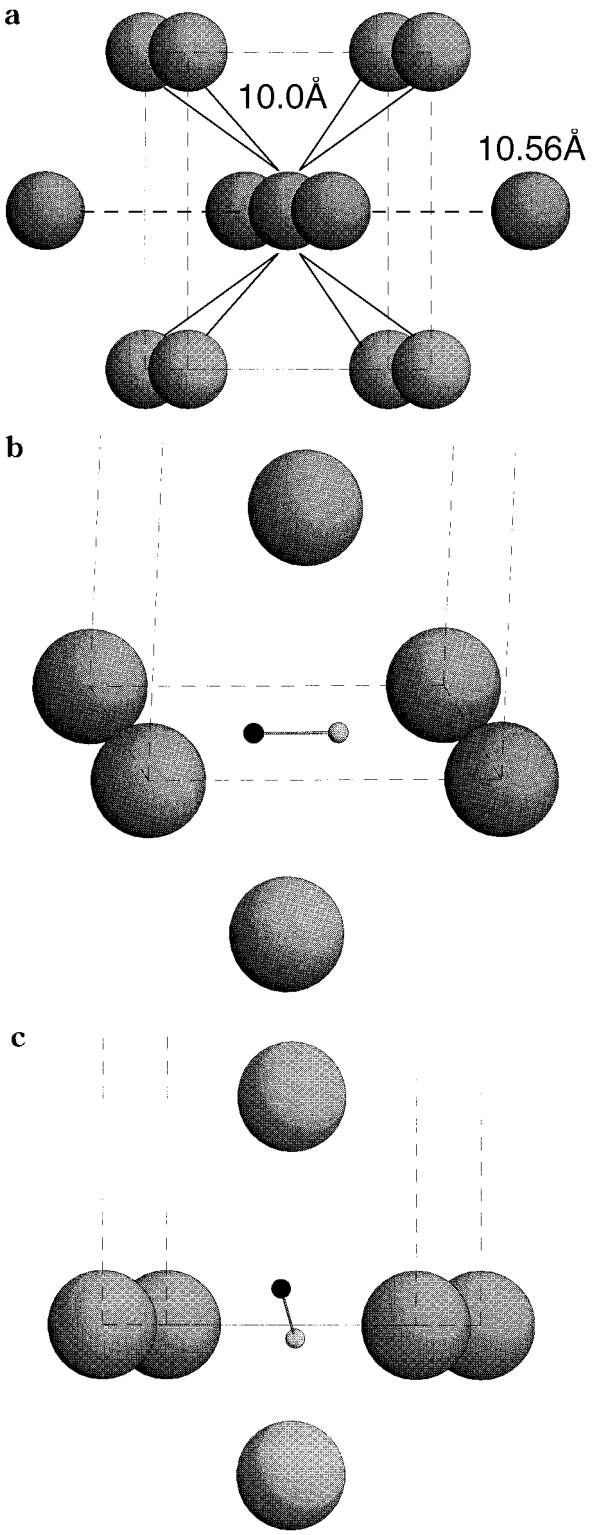

Figure 14. (a) The nearest neighbors of a C_{60}^{3-} anion in $(NH_3)K_3C_{60}$.[89] In the $Fm\bar{3}m$ parent phase K_3C_{60}, all 12 neighbors are at a distance of 10.0 Å from a C_{60}^{3-} anion. In $(NH_3)K_3C_{60}$ the linear $(K-NH_3)^+$ complex on the octahedral site pushes the four neighbors in the *ab* plane to a distance of 10.56 Å (dashed lines), leaving only eight fulleride anions at 10.0 Å at the vertexes of a cuboid (solid lines). The *c*-axis is vertical ($a = 10.56$ Å, $c = 13.68$ Å). (b) The linear $K-NH_3$ complex is disordered over the *fcc* ⟨110⟩ directions, producing expansion of the octahedral site in the *ab* plane in $(NH_3)K_3C_{60}$ and lowering the symmetry from *fcc*. (c) The $Na-NH_3$ complex in $A_2Na(NH_3)C_{60}$[87] is directed along the ⟨111⟩ directions, allowing the phase to retain cubic symmetry.

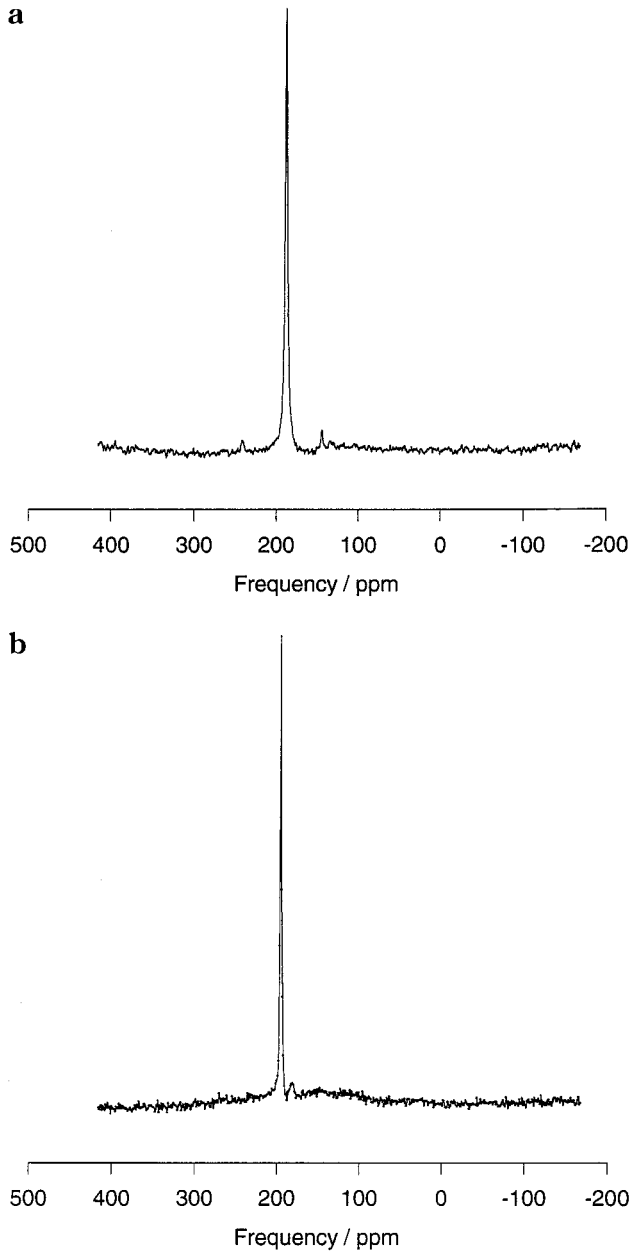

Figure 15. (a) ^{13}C MAS NMR spectrum of K_3C_{60} at 298 K ($\delta = 186$ ppm). (b) ^{13}C MAS NMR spectrum of $(NH_3)K_3C_{60}$ at 298 K ($\delta = 193$ ppm). The increased chemical shift is assigned to the larger Knight shift produced by the narrower bands in the expanded fulleride.[91]

ever.[90,91] The Knight shift (Figure 15) of 43 ppm lies between that of K_3C_{60} (37 ppm) and the equally expanded Rb_3C_{60} (47 ppm), indicating that the expansion reduces the t_{1u} bandwidth and enhances $N(E_f)$ by 15%, although to a lesser extent than in the cubic Rb_3C_{60}. The N_χ measured by EPR is similar to that for K_3C_{60}, also indicating that t_{1u} degeneracy lifting reduces the number of states at E_f compared with Rb_3C_{60}.

The vanishing of the EPR signal in $(NH_3)K_3C_{60}$ (Figure 16) below 40 K is consistent with a metal−insulator transition.[90,91] Recent muon spin relaxation (μSR) measurements show the development of a heavily damped oscillation below 40 K, indicating that antiferromagnetic order develops at the transition.[129] This result is extremely significant because it is the first direct demonstration of a close relationship between the

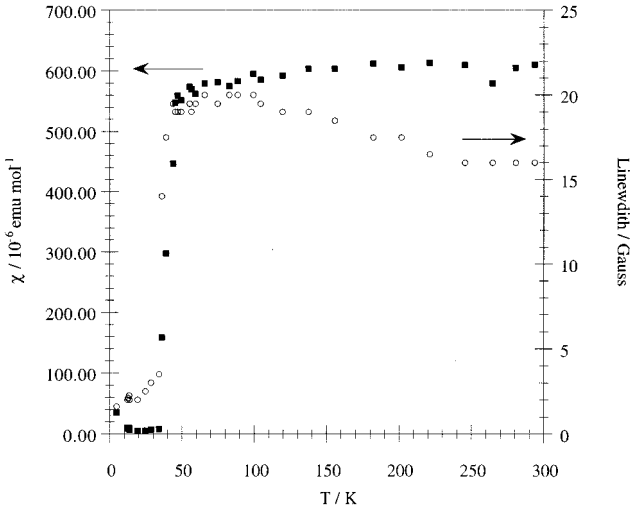

Figure 16. EPR measurements of magnetic susceptibility (closed squares) and peak-to-peak line width (open circles) of $(NH_3)K_3C_{60}$.[91]

antiferromagnetic and superconducting ground states in C_{60}^{3-} systems. The requirement to suppress antiferromagnetism to produce superconductivity in the high T_c copper oxides is well documented. Application of 15 kbar hydrostatic pressure suppresses the 40 K metal−insulator transition and induces superconductivity in $(NH_3)K_3C_{60}$ at 28 K.[92] Antiferromagnetism competes with superconductivity in the tetragonally distorted structure, perhaps being favored by reduction in point symmetry of C_{60}^{3-} and narrowing of the t_{1u} bandwidth, as compression makes the structure more isotropic.[92] The role of orbital degeneracy in combatting the Mott−Hubbard transition may be significant here.

3.2. Chemistry of Ammoniated Fullerides. The examples just discussed indicate the extent to which the electronic properties of a fulleride can be controlled by the size and shape of a metal−ammonia complex cation and the resulting effect on cation disorder or fulleride packing. Much more dramatic distortions of the *fcc* structure are, however, possible and the synthesis of new ammoniated fullerides with a range of different anion packings has recently been demonstrated. These new structures may hold a rich array of physical properties.

Ammoniated fullerides with *bcc* rather then *fcc* packings may be prepared either from liquid ammonia or by reaction of ammonia gas with an alkali metal intercalated host. $Na_3(NH_3)_6C_{60}$[93] and $Li_3(NH_3)_4C_{60}$[94] both adopt a *bcc* structure. In the sodium compound, there are essentially linear $(NH_3)_2Na^+$ units, formed by NH_3 molecules occupying the tetrahedral sites (occupied by potassium cations in K_6C_{60}) and sodium cations displaced from the centers of the octahedral sites. Antisite disorder of sodium and nitrogen over both sites is indicated by synchrotron X-ray work,[95] although not by neutron powder diffraction, which finds extensive ND_3 orientational disorder coupled with positional disorder of both moieties.[93] This phase is of significance because it adopts the same anion structure as the superconductor Cs_3C_{60} yet is nonsuperconducting with a 3^- anion charge.

The large volume per fulleride anion, according to EPR and superconducting quantum interference device (SQUID) measurements,[96] produces *localized* electron behavior, suggesting that the Mott−Hubbard ground state as well as the itinerant electron antiferromagnetism found for $(NH_3)K_3C_{60}$, are close to those of the superconducting one. The synthesis of this phase using both solid Na_3C_{60}[93] and a liquid ammonia method[95] is evidence for the existence of an *fcc* phase with a composition close to Na_3C_{60} (see Section 5). The interfulleride separation of 10.5 Å and the volume per C_{60}^{3-} anion of 885 Å^3 are the largest yet found and are apparently sufficient to provoke localization of the t_{1u} electrons. A simple estimate of the bandwidth reduction in $Na_3(NH_3)_6C_{60}$ is to 40% of that for K_3C_{60}, allowing an estimate of a lower bound for the value of U required to produce electron localization in A_3C_{60} compounds.

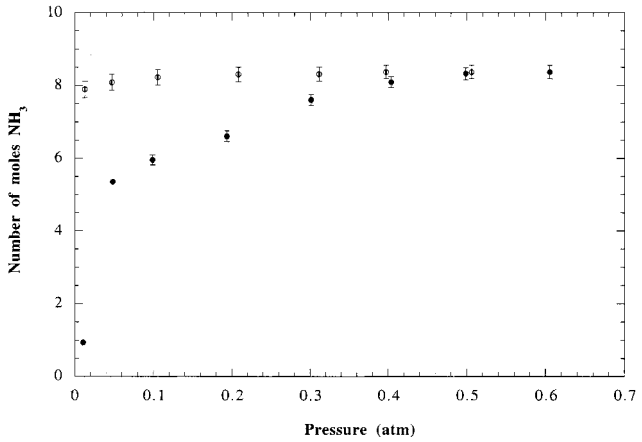

Figure 17. The ammonia uptake isotherm of $(NH_3)_8Na_2C_{60}$ at 298 K. The hysteresis between the uptake (filled symbols) and desorption (open symbols) legs is due to slow intercalation kinetics.

Scheme 1. Topotactic Room Temperature Solid−Gas Reaction between Na_2C_{60} and NH_3

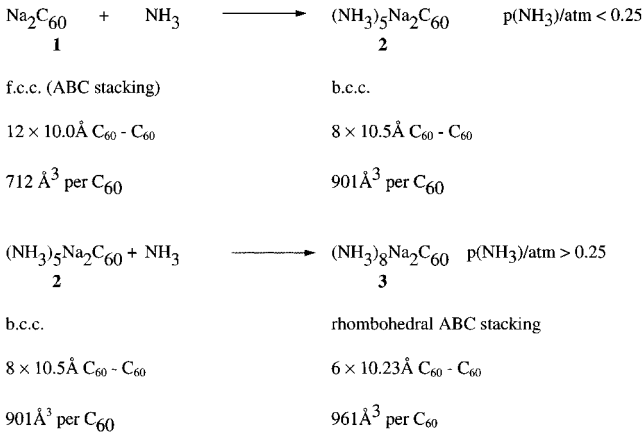

3.2.1. $(NH_3)_8Na_2C_{60}$—A New Fulleride Structure Type Based on Expanded Close Packing. All the sphere packings discussed above are achievable without the use of ammonia to complex the alkali metal cations. In contrast, the reaction of Na_2C_{60} with ammonia affords a quite new structure.[95,97] Scheme 1 shows the sequence of topotactic reactions occurring between gaseous ammonia and the *fcc*-packed ($Pa\bar{3}$ orientational order) Na_2C_{60} **1**, yielding the final product rhombohedral $(NH_3)_8Na_2C_{60}$ phase **3**.

Figure 17 shows the ammonia uptake isotherm of Na_2C_{60}, corresponding to the reactions shown in Scheme 1. The inflection at $n = 5.3$ corresponds to the formation

of a *bcc* phase **2** similar to $(NH_3)_6Na_3C_{60}$ (but with an orthorhombic superstructure). The endpoint at $n = 8$ corresponds to the formation of a phase with a new rhombohedral structure ($a = 12.221$ Å, $c = 22.296$ Å). The interesting chemical point is that although the volume per C_{60}^{2-} increases between $n = 5$ and $n = 8$, as expected, the closest interfulleride separation *decreases*. Isotropic expansion of the twelve 10.0 Å contacts in Na_2C_{60} to eight nearest neighbors at 10.5 Å in the $n = 5$ phase occurs before the increased ammonia loading produces a combination of a further increase in volume per anion to 961 Å^3 with a *contraction* in the nearest neighbor distance from the *bcc* phase to 10.24 Å (six molecules), with six more distant neighbors at 12.22 Å. The closest C...C distances therefore increase despite the overall expansion of the solid. This unusual feature, combining an interfulleride separation equal to that in Rb_3C_{60} with a very expanded fulleride packing, prompted a detailed investigation of the structure combining neutron and X-ray powder diffraction analysis.[97]

The structure consists of an ABC stacking of layers in which each C_{60}^{2-} has six neighbors within the layer (i.e., an axial elongation of *fcc* along one of the 3-fold axes of the unit cell). The *fcc* packing of the Na_2C_{60} starting material can be represented as an R-centered hexagonal cell with $a = 10.0$ Å and $c = 24.49$ Å. Each C_{60} has 12 nearest neighbors at the vertexes of a cuboctahedron, with six near neighbors in the hexagonal *ab* plane in one close-packed layer and six from the neighboring layers arranged octahedrally. In $(ND_3)_8Na_2C_{60}$, the six neighboring molecules in the *ab* plane have been displaced to 12.22 Å away, strongly expanding the formerly close-packed layers. The ABC sequence along the rhombohedral *c*-axis is retained; the now-expanded layers are stacked to maintain the close-packed contacts *between* the layers, because the interlayer separation is 10.23 Å, which corresponds to the anions remaining in electronic contact only between the layers (Figure 18). The structure is thus an *fcc* packing in which the close-packed layers have been exploded by >2 Å, whereas the *inter*layer contacts remain little changed, making it a very unusual derivative of a sphere packing. This structure is clearly one which cannot result from the insertion of spherical counterions into the fulleride array.

The structure arises from a hierarchy of weak intermolecular interactions, with the coordination of ND_3 to Na^+ producing pseudo-tetrahedral complexes, with one "axial" ND_3 (Na−N vector oriented along the layer stacking direction) and three "equatorial" ND_3 molecules (Figure 19(a)). In Figure 19(b), the location of the complexes in the ABC stacking sequence of the expanded layers is shown in relation to the *fcc* interstitial sites. The complexes occupy two sites produced by displacement of 1.91 Å away from the center of the octahedral site along the stacking axis, leaving each C_{60}^{2-} surrounded by six $Na(ND_3)_4^+$ complexes, three below and three above the fulleride layer.

These $(ND_3)_4Na^+$ complexes determine the fulleride packing through both attractive and repulsive C...D interactions. The layer expansion is driven by close C...D contacts between the six-membered rings of the C_{60}^{2-} anion and the equatorial ammonia molecule,

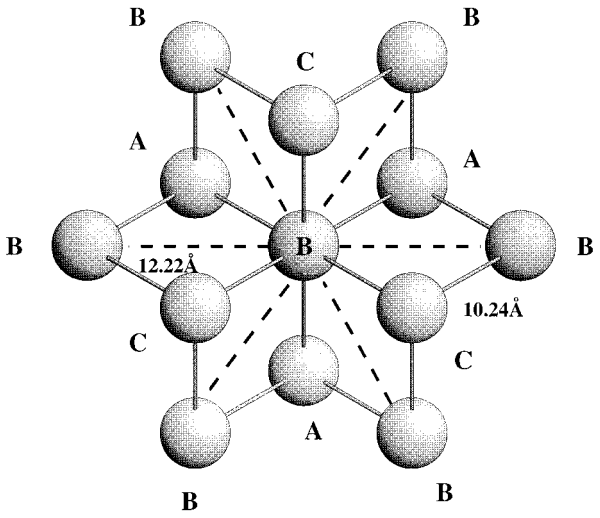

Figure 18. The expanded close-packed structure of $(ND_3)_8Na_2C_{60}$, viewed along the stacking direction. The 10.24 Å interlayer contacts are shown as hollow lines to the six nearest neighbors of the central B layer fulleride anion ($z = 0$), to the neighboring A ($z = -1/3$) and C ($z = +1/3$) layers. The six 12.22 Å intralayer nearest-neighbor distances within the B layer are coincident with the *a* and *b* cell vectors and represented by the thick dotted lines.[97]

which is strongly indicative of the formation of a hydrogen bond with the π-electrons of the C_{60}^{2-} anion (Figure 20). Hydrogen bonds of the type X−H...π (X = N,O), where π is an electron-rich system such as alkene, alkyne, or phenyl, are well-established.[98,99] Each C_{60}^{2-} makes 12 of these closest contacts, to two ND_3 molecules from each neighboring $Na(ND_3)_4^+$ complex, via 12 of its hexagonal rings. The six-membered rings on the fulleride anion are able to form these weak interactions because they are relatively electron rich and sterically unhindered.

These hydrogen-bonding interactions expand the layers; that is, each of the six interfulleride 12.23 Å distances within the layer is bridged by four of these N−D... π hydrogen bonds (shown as dark lines in Figure 21), forming a hexagonal network. The 3-fold axes of the "axial" ammonia molecules are aligned with those of the C_{60}^{2-} anions in neighboring layers, allowing the much closer *inter*layer contacts. The attractive and repulsive C...D interactions thus combine to produce the unusual six plus six "expanded close-packed" environment of the fulleride anion.

Although fulleride molecular dynamics have been well studied in the pure A_3C_{60} and A_6C_{60} phases, there is much less known about the interplay of the motions of the complex cations and anions in the increasingly important ammoniated phases. The molecular dynamics within $(ND_3)_8Na_2C_{60}$ are complex and both ^{13}C and ^2H NMR probes show the influence of the cation−anion interaction.[97] The ^2H spectra indicate ND_3 reorientation about its C_3 axis at $>10^8$ Hz persists to 150 K and that there are a distribution of barriers to the isotropic reorientation of the complex itself. The wide-line ^{13}C NMR spectra at 298 and 132 K are shown in Figure 22. The single resonance due to isotropic anion reorientation at 298 K becomes a powder pattern from an axially symmetric shift tensor at 132 K. The line shapes do not precisely correspond to those expected for simple slowing down of an icosahedral reorientation, suggesting

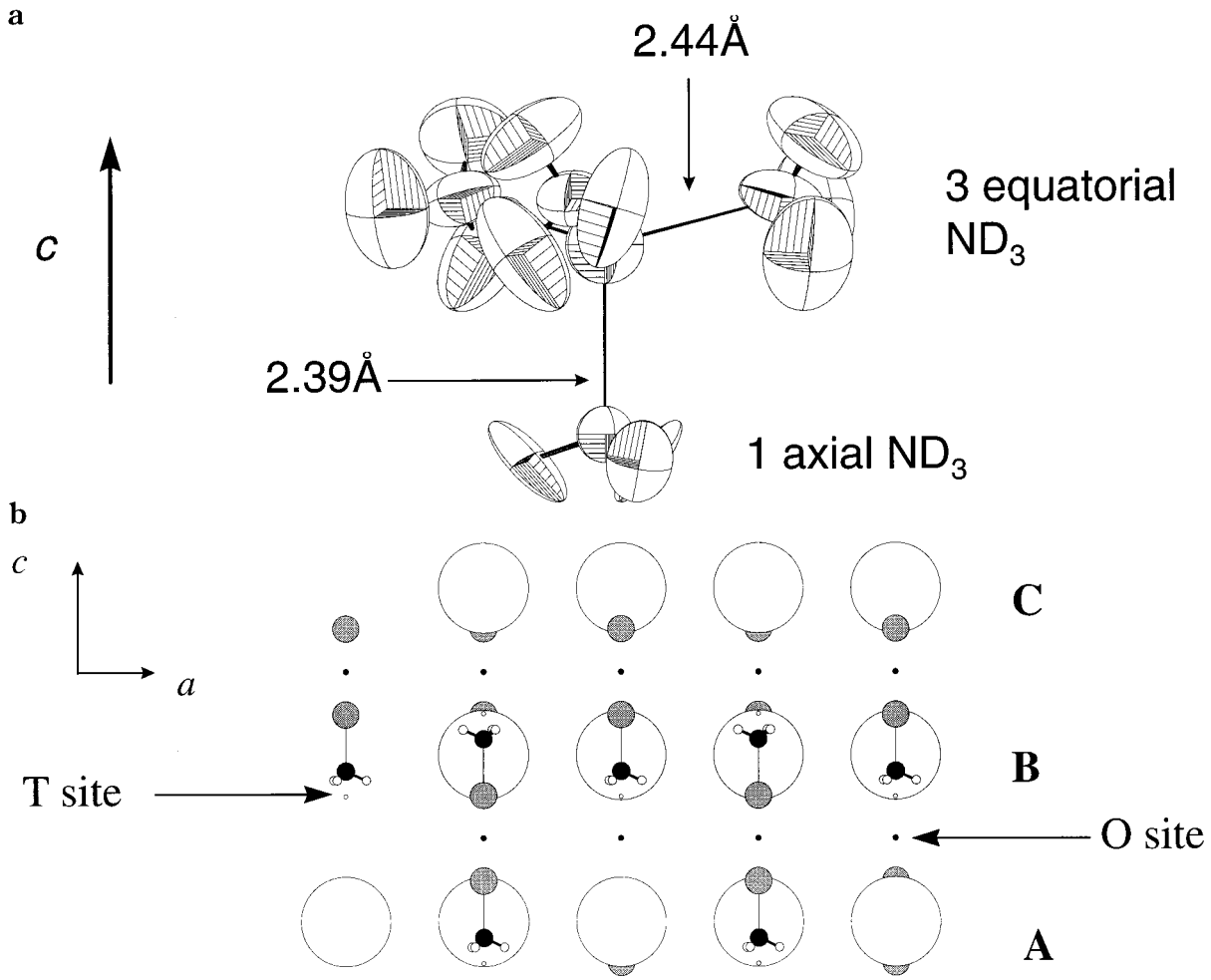

Figure 19. (a) The $Na(ND_3)_4^+$ complex from the structure of $(ND_3)_8Na_2C_{60}$ in $R\bar{3}$ symmetry, showing the two crystallographically distinct ammonia molecules. (b) The ABC stacking sequence of expanded fulleride layers in $(ND_3)_8Na_2C_{60}$. The fulleride anions are represented as spheres. The formation of the complex cations is illustrated by depiction of a subset of the axial ammonia molecules and sodium cations. The sodium cations and axial ammonia molecules are seen to be displaced from the tetrahedral (open small spheres) and octahedral (black small spheres) sites, with an ammonia molecule from the AB gap coordinating a sodium cation in the BC gap.[97]

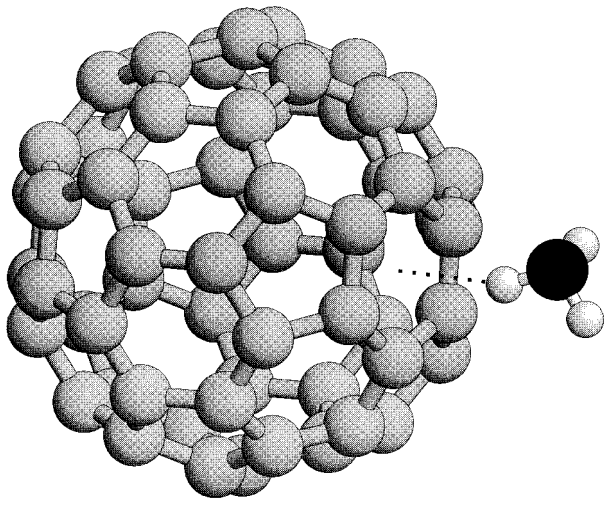

Figure 20. The N−D...π interaction in $(ND_3)_8Na_2C_{60}$ between the equatorial ND_3 and a six-membered ring of the C_{60}^{2-} anion: the deuterium is located 2.61 Å above the centroid of the hexagon.

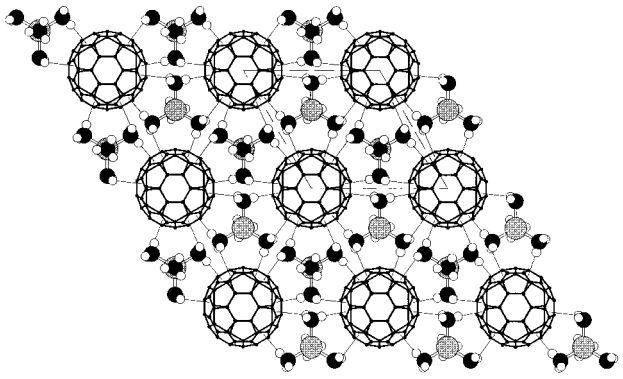

Figure 21. The weak hydrogen bonds shown in Figure 20 between the equatorial ammonia and the fulleride anions form an extended network within the expanded fulleride layers. The thin lines show the hexagon centroid over which the deuterium atoms lie. Each equatorial ammonia molecule interacts via two deuterium atoms with two C_{60}^{2-} anions separated by 12.22 Å. Fulleride anions from neighboring layers are located over the axial ammonia molecules. The sodium cations are shown as gray.[97]

that at room temperature, where the signal observed is isotropic, two different motions are occurring: axially symmetric reorientation of the C_{60}^{2-} by 3-fold jumps of the molecules around the C_3 axis at the centroid of the six-membered rings (motion (a) in Figure 22(c)), and jumps between equivalent axis orientations (motion (b)

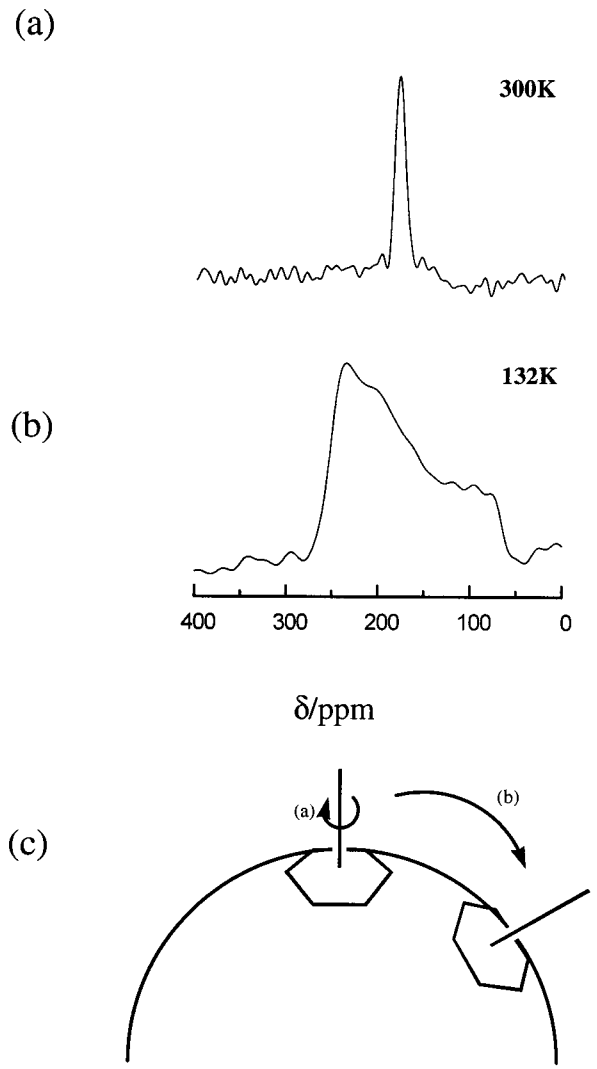

Figure 22. The ^{13}C wide-line NMR spectra of $(ND_3)_8Na_2C_{60}$ at (a) 300 K and (b) 132 K. (c) Indication of the two reorientational motions of the C_{60}^{2-} anion consistent with the line shape. Process (b), involving the interchange of the six-membered rings, is frozen at 132 K.

in Figure 22c) leading to fully isotropic reorientation. On cooling, the interconversion of the symmetry inequivalent hexagons (motion (b)) freezes out first, leaving only the C_3 reorientation (motion a). The 298 K ^{13}C T_1 is very short (10 ms) compared with that of Na_2C_{60} (425 ms) and $(ND_3)K_3C_{60}$ (102.5 ms), and temperature-independent. The averaging of the hydrogen bonding of the C_{60}^{2-} ions to the quadrupolar deuterium nucleus by isotropic anion reorientation is the probable source of this efficient relaxation. The correlation between the short ^{13}C T_1 and the close C...D contacts found in the diffraction studies is further evidence for specific hydrogen bonding interactions being responsible for the structure of $(ND_3)_8Na_2C_{60}$.

The example of $(ND_3)_8Na_2C_{60}$ shows that interactions with nonspherical counterions can produce new fulleride structures in which the anions remain in electronic contact. The use of the X−H...π bonding to control fulleride structure may prove to have wider application. This structure has sufficiently short inter-C_{60} contacts to allow delocalization of the t_{1u} electrons, motivating the search for isostructural C_{60}^{3-} phases.

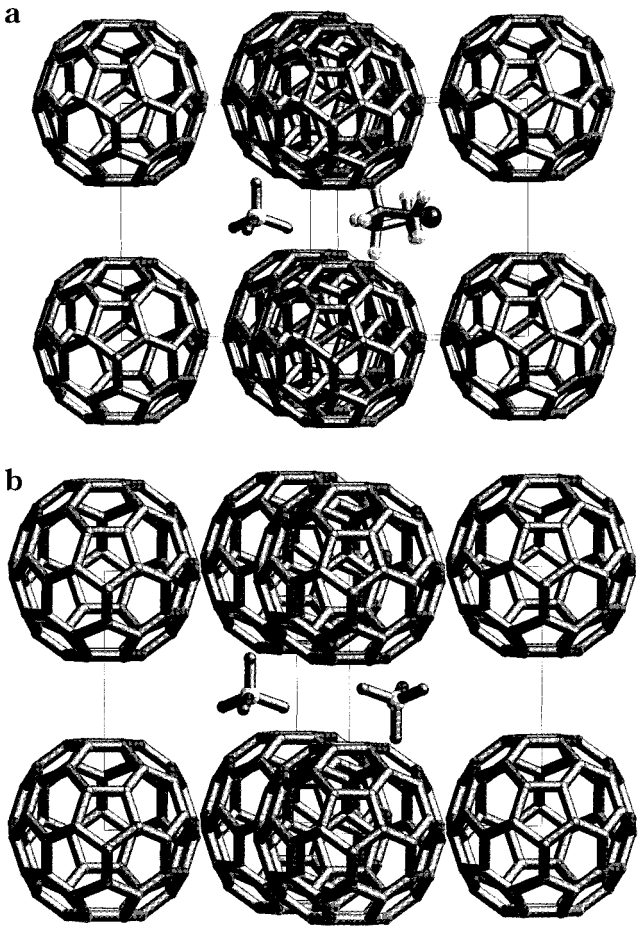

Figure 23. The structures of primitive hexagonal tetraalkylammonium fullerides. (a) $(THF)(CH_3)_4NC_{60}((CH_3)_4N)_2C_{60}$; and (b) $((CH_3)_4N)_2C_{60}$.

4. Alkylammonium C_{60} Phases

The preparation of C_{60}^- and C_{60}^{2-} salts of the tetramethylammonium cation was recently achieved by Douthwaite.[100] Both $((CH_3)_4N)_2C_{60}$ and $(THF)(CH_3)_4NC_{60}$ salts adopt a primitive hexagonal structure, with an AAA stacking of close-packed C_{60} layers in contrast to the close-packed stackings discussed so far (Figure 23). This primitive hexagonal structure is also found for $(P_4)_2C_{60}$,[101,102] which also contains two large tetrahedral groups per C_{60} molecule. The important crystal chemical point is that the presence of two large groups (two $(CH_3)_4N^+$ cations, or one $(CH_3)_4N^+$ cation and one solvating THF, or two P_4 units) appears to favor the primitive stacking sequence, which contains two large trigonal prismatic sites per anion, compared with the single large octahedral site found in the close-packed structures. The instability of all the AAA stacked materials to attempts to remove 50% of the species in the trigonal prismatic sites suggests that the complete filling of the large interstitial sites in the array is key to its stability. The C_{60}^- phase is stable to polymerization and appears to be a highly correlated metal above 230 K, which is consistent with eight 10 Å interfulleride contacts. A sharp reduction in the susceptibility below 230 K is consistent with a metal−insulator or metal−metal transition coincident with a structural transition, associated with a pronounced slowing of the anion reorientational dynamics indicated by ^{13}C NMR.

5. Sodium Fullerides

Following initial reports detailing phase stability in the Na_xC_{60} field,[76] an almost complete range of *fcc* solid solutions for $2 < x < 10$ due to multiple occupancy of the octahedral site by sodium,[36,76,103] the absence of superconductivity at any composition, and only one report of metallic behavior (in Na_2C_{60}),[104] there was a lull in studies of these phases. Recent work, both theoretical and experimental, has shown that there are many questions to answer and intriguing properties, in particular relating to the interpretation of the observed structures in simple chemical bonding terms.

Na_2C_{60} adopts the fluorite structure, with essentially complete occupancy of the tetrahedral sites by sodium. The vacant octahedral site allows this phase to act as a host for postsynthesis intercalation of mercury from the vapor phase to form $Na_2Hg_yC_{60}$ ($y \leq 0.25$).[105] In contrast to alkali metal species on the octahedral site, structural and NMR data indicated that the inserted Hg transfers little charge to the C_{60}^{2-} anions.

A new Na_4C_{60} phase[106] has been prepared, with a unique polymer structure, based on layers of polymer formed by each C_{60} making four single bonds to its neighbors. The phase is metallic, albeit with a strongly temperature-dependent magnetic susceptibility.

Aside from the well-characterized Na_2C_{60}, the phase relations themselves remain a matter of controversy: Na_3C_{60} was not found in a recent X-ray study of Na_xC_{60} phases prepared at 200 °C.[106] The absence of solid solution between $x = 2$ and $x = 3$ is in conflict with previous X-ray studies[36,76] and typical of the uncertainty that still surrounds this phase diagram. The most complete understanding of the thermodynamics of phase relations in this system is offered by a 600 K electrochemical study that indicates a miscibility gap in Na_xC_{60} for $0 < x < 2$, solid solution for $2 < x < 3$, and a further miscibility gap until $x = 3.7$.[107] Thin films studied by Raman,[108] electron diffraction, and EELS[109] also show solid solution, with Na_4C_{60} adopting an *fcc* rather than a polymeric structure.

There appears to be a consensus on the existence of *fcc* structures for $x \geq 6$, with several confirmations of the $x = 6$[106,110] and $x \approx 10$[71,109,111] phases. Multiple occupancy of the octahedral site in $Na_{6+x}C_{60}$ has attracted attention since the first reports of Na_4[76] and Na_{9-x}[103] units from X-ray powder diffraction attracted theoretical criticism[112] for underestimating the Na−Na distances, calculated as a minimum 3.2 Å. A recent combined ^{13}C and ^{23}Na NMR study of Na_6C_{60} confirms the Na_4 unit on the octahedral site.[110] The tetrahedral sodium cations occur at the same ^{23}Na chemical shift (73 ppm from aqueous NaCl) as in Na_2C_{60}, whereas the 147 ppm "octahedral cluster" resonance has twice the intensity of the T resonance, consistent with an Na_4 group. The marked shifts from Na^+(aq) were interpreted as indicating incomplete charge transfer to C_{60}, particularly from the sodium species occupying the octahedral site. This interpretation is backed up by Raman measurements and the 176 ppm ^{13}C shift, which is 20 ppm downfield from the *bcc* A_6C_{60} phases from the heavier alkalies.[113] The NMR evidence implies a reduced occupancy of the t_{1u} orbitals and incomplete Na ionization, with a smaller positive charge on the octahedral "cluster" sodium cations.

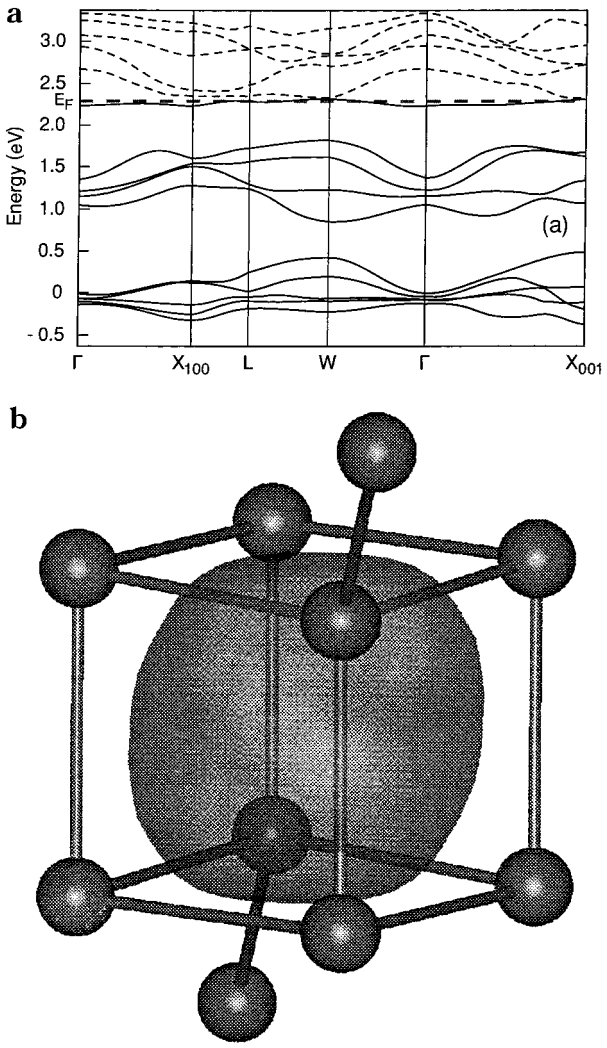

Figure 24. The electronic structure of $Na_{10}C_{60}$. (a) Band structure. The Fermi level marked by E_f lies in the t_{1g} states. The band below E_f at the Γ point, above the filled t_{1u} bands, is the "*O* void" state trapped by the Madelung potential of the Na_8^{8+} unit. (b) Probability density of the "*O* void" state at the Γ point of the Brillouin zone. Reproduced with permission from ref 111.

This chemically appealing picture is challenged by a combination of electron energy loss spectroscopy (EELS) and LDA/Car-Parrinello calculations[111] (Figure 24). EELS is consistent with a constant, nearly complete degree of Na ionization over the $4 < x < 10$ range, with the transferred electrons entering the t_{1u} levels of C_{60} for $x < 6$. However, the C 1s absorption data do not change between the Na_6C_{60} and Na_8C_{60} compositions. These data are interpreted as indicating that, although Na is still ionized, the electrons do not enter the t_{1g} "LUMO + 1" level. The radical interpretation suggested by theory does *not* involve Na−C covalency, but places the two electrons at the center of the octahedral (O) site, trapped by the Madelung potential of the Na^+ cations in the Na_8 unit, but not in Na-derived orbitals. $Na_{10}C_{60}$ has an apparent charge of C_{60}^{8-}, consistent with subsequent occupation of the t_{1g} levels once the "cluster trap" states are occupied, leading to a theoretical prediction of metallic behavior. Interestingly, the relaxed $Na_{10}C_{60}$ structure[111] is calculated to be a highly irregular Na_8 parallelepiped, with Na−Na distances between 3.3 and 3.9 Å and pronounced displacement of

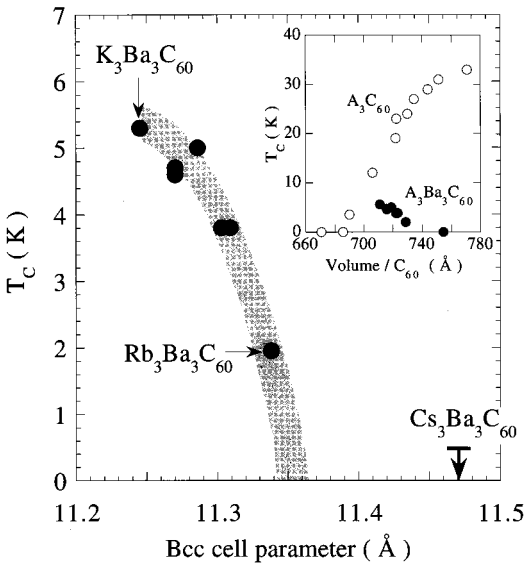

Figure 25. Variation of T_c with *bcc* unit cell parameter in the $A_3Ba_3C_{60}$ phases. The dependence is opposite to that found for the A_3C_{60} phases shown in Figure 2. Reproduced with permission from ref 114.

the tetrahedral Na from the site center to give a 3.1 Å contact to the sodiums occupying the O sites. The combined theoretical and experimental image of nonrigid band behavior in systems in which the t_{1g} levels are formally occupied is clear.

6. Superconductivity in the Half-filled t_{1g} Band—$A_3Ba_3C_{60}$

The t_{1g} "LUMO + 1" level of C_{60} offers the same symmetries for electron−phonon coupling as the t_{1u} level, because the $t_{1u}\otimes t_{1u}$ and $t_{1g}\otimes t_{1g}$ direct products are equivalent. The recent syntheses of $A_3Ba_3C_{60}$ phases[114] (A = K, Rb, Cs) with a formal C_{60}^{9-} charge and half-filling of the t_{1g} band allows this correspondence between the t_{1u}^3 and t_{1g}^3 configurations to be probed experimentally. The synthesis involves Ba_3C_{60}, which is a vacancy-ordered derivative of the *bcc* A_6C_{60} structure with half of the cation sites empty (A15 structure), as an intercalation host, taking up three alkali metal cations at 250° to form a cation-*dis*ordered $A_3Ba_3C_{60}$ phase isostructural with K_6C_{60}. The half-filled t_{1g} band does produce superconductivity (T_c = 5.6 K for $K_3Ba_3C_{60}$), but the insertion of larger A^+ cations reduces T_c, contrary to the behavior of the C_{60}^{3-} phases (Figure 25). Normal-state susceptibility measurements show that the density of states at the Fermi level is about half that of the A_3C_{60} compounds, suggesting broader bands. McMillan equation analysis of the dependence of T_c on N_χ indicates that the pairing phonon has a much reduced energy of 320 K.

7. Higher Fullerenes

Although C_{60} is only one member of the C_{2n} ($n \geq 10$) fullerene family, it is by far the most intensively studied because of its preponderance in current fullerene syntheses. It is natural to ask whether the striking range of electronic properties observed for the C_{60} fullerides has any analogy in the intercalates of the higher fullerenes.

The extensive metal intercalation chemistry of C_{60} can be attributed to the low energy of its frontier orbitals, conferring a high degree of electronegativity on the molecule.[115] The linking feature of the geometric structures of the family of fullerenes, the presence of 12 pentagons plus an arbitrary number of hexagons, also gives each fullerene six low-lying empty orbitals in analogy to the t_{1u} LUMO and t_{1g} "LUMO + 1" levels of C_{60} itself. This ability to accommodate up to 12 additional electrons may be thought of as each five-membered ring taking up one electron to form a six π-electron unit. Therefore, each higher fullerene might also be expected to display an extensive intercalation chemistry. The details of the crystal structure can be expected to depend on the molecular point symmetry of the fullerene in question, and with recent theoretical and experimental work focusing attention on the key role of the degeneracy of the t_{1u} C_{60} LUMO in avoiding the seemingly inevitable Mott-Hubbard transition at the C_{60}^{3-} charge. The wide variation in the degeneracies of these six low-lying orbitals, again controlled by fullerene molecular symmetry,[116] can be expected to confer a wide variety of electronic properties on higher fulleride intercalates. However, experimental work on these systems remains sparse because there are severe obstacles; for example, many of the higher fullerenes occur as structural isomers that are extremely difficult and time-consuming to separate from each other.

C_{70} has only one isolated pentagon isomer, with D_{5h} symmetry, and has thus been the most extensively studied higher fullerene. The frontier orbitals of C_{70} are two closely spaced a_1'' (LUMO and precisely nonbonding in Huckel theory) and e_1'' (LUMO + 1) levels (there are no 3-fold degenerate representations of D_{5h}). These two levels are predicted to be close in energy[117] and the electronic ground states of C_{70}^{n-} anions can be expected to be even more complex than the C_{60}^{n-} cases. Experimentally, the K_xC_{70} phase diagram is the best-studied, revealing rock-salt K_1C_{70}, *bct* K_4C_{70}, *bcc* K_6C_{70}, and *fcc* K_9C_{70} phases.[118,119] Significantly, the K_3C_{70} composition disproportionates below 440 K,[118] making it hard to evaluate the significance of the conclusion from electron spectroscopies on thin film samples that C_{70}^{n-} fullerides are nonmetallic. Further synthetic work to prepare C_{70}^{3-} phases stable to lower temperature is called for. The K_9C_{70} phase is suggested to have a similar structure to *fcc* $Na_{6+x}C_{60}$, although two different (x,x,x) positions, corresponding to two interpenetrating tetrahedra rather than a cube, are used to describe the occupancy of the octahedral site.[119] There is as yet no detailed treatment of the C_{70}^{n-} orientation in any of these phases. Fully ordered structures would have monoclinic symmetry, and theory indicates that the orientational disorder required by the reported crystal symmetries will have a profound effect on the properties.[120] A detailed transport study indicates that K_4C_{70} films are weakly localized metals, with the absence of superconductivity attributed to weaker electron−phonon coupling than in the C_{60} case.[121] It is clear that the near-spherical shape and LUMO degeneracy of C_{60} are not present in C_{70}, and this may be a possible explanation for the differences in structural chemistry and electronic properties.

Using the simple similarity criteria of near-spherical shape and LUMO degeneracy to guide the search for

analogies of the intercalation chemistry of C_{60} leads to the D_{2d} isomer of C_{84}. There are actually 24 isolated pentagon isomers of C_{84},[116] but current syntheses yield a 2:1 mixture of the D_2 (majority) and D_{2d} (minority) isomers. C_{84}-D_{2d} is nearly spherical ($r_{max}/r_{min} = 1.01$) and has a doubly degenerate LUMO (Figure 26(a)).

PES studies of vacuum deposited films of the 2:1 mixture of D_2 and D_{2d} isomers of C_{84} gave evidence for a range of phases, without any indication of metallic behavior.[122−124] The intrinsic narrow bandwidth of fullerides combined with the larger disorder potential and vibronic barrier to electron transfer arising from the differing electronic structure of the two isomers could be expected to give rise to polaronic or Anderson localization. The recent separation of the two C_{84} isomers by HPLC methods[125] is therefore an essential prerequisite to the understanding of the extent to which analogies to C_{60} are possible. This important development has allowed the isolation and structural analysis of $K_{8+x}C_{84}$ *fcc* phases for the D_2, D_{2d}, and 2:1 mixed isomer host solids.[126] The structures, derived from synchrotron X-ray powder diffraction on <0.4 mg samples, appear similar to $Na_{6+x}C_{60}$, but when examined in detail, show how the lower point symmetry higher fullerenes can be partially orientationally ordered by cation−anion contacts even in cubic structures.

The C_{84}-D_{2d} molecular symmetry is lower than the O_h point symmetry of the site occupied in the crystal by the C_{84} anion and therefore orientational disorder is inevitable. Partial orientational order is achieved by alignment of the $\bar{4}$ axis of the molecule with the cube axes; there are then two possible orientation choices. The normals to the mirror planes cutting through the 6:6 bonds can be aligned with the ⟨100⟩ directions ($\bar{4}m2$ symmetry) or along the ⟨110⟩ face diagonals ($\bar{4}2m$ symmetry; Figure 26(b) and (c)). Refinement clearly indicates that the $\bar{4}2m$ orientation, with the 6:6 bonds rotated 45° from the C_{60}^{3-} orientation in K_3C_{60} (Figure 3(a)), is preferred for both pure D_2 and D_{2d} host isomers and also the mixed isomer host. This result is due to the avoidance of over-close contacts between the potassium cation on the tetrahedral site and the carbon atoms. In this orientation, the tetrahedral potassium cation is located directly over the centroids of four six-membered rings from the neighboring C_{84} anions.

The partial orientational order occurs because the shapes of both the D_2 and D_{2d} isomers are almost compatible with cubic symmetry, despite the absence of a 3-fold axis. The orientationally ordered molecules have a hexagon centroid located along the $Fm\bar{3}m$ C_3 axes (the cube diagonals). This is not a C_3 axis of the C_{84} molecule itself, because this hexagon is surrounded by two pentagons and four hexagons (unlike the more symmetrical C_{60} in which it is a true C_3 axis), but can be seen as a 'pseudo-C_3' axis. The C_3 operation in $Fm\bar{3}m$ superimposes the pentagons and hexagons around the hexagon perimeter, while still maintaining the hexagon centroid along the [1 1 1] direction, allowing acceptable K...C contacts.

The interstitial sites in the *fcc* anion array are occupied in a very similar way to the $Na_{6+x}C_{60}$ phases. The tetrahedral site is almost fully occupied and there is multiple potassium occupancy of the octahedral site. Approximately 25% of the octahedral site center and

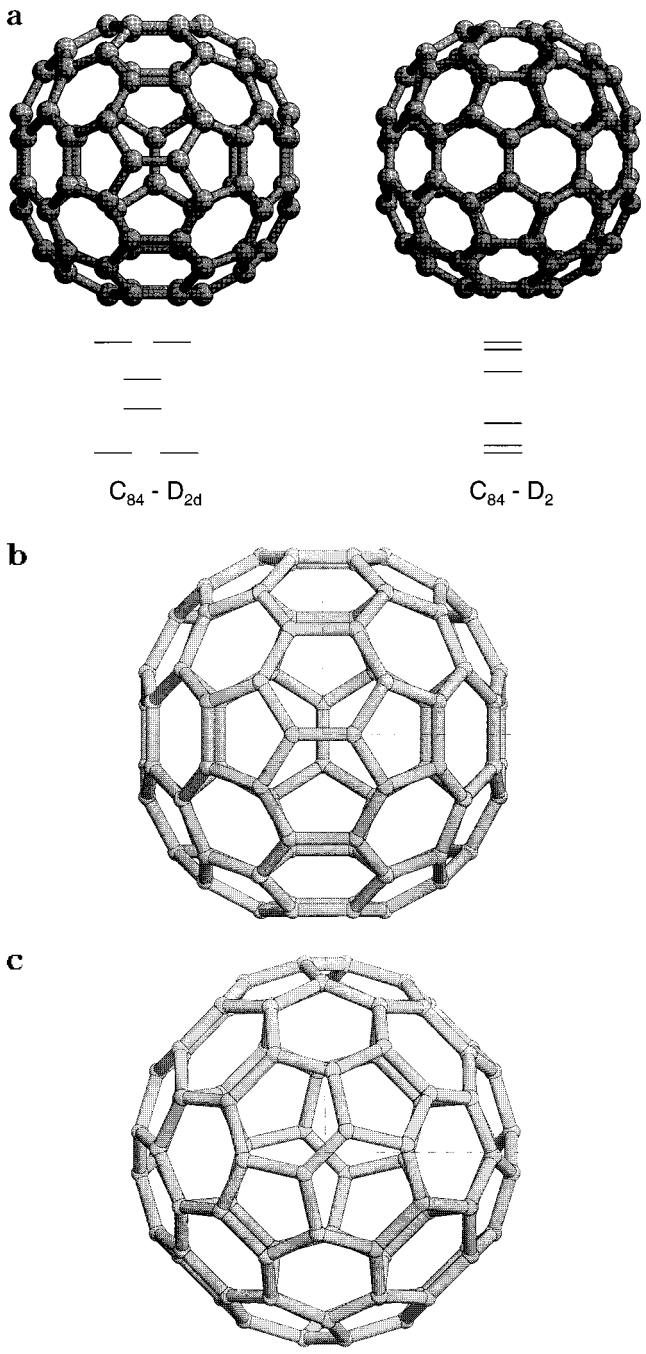

Figure 26. (a) The D_2 and D_{2d} isomers of C_{84} with the six LUMOs of each molecule. Note the degeneracy of the D_{2d} LUMO. There are two possible (partially ordered) orientations of the C_{84}−D_{2d} isomer with respect to the symmetry operations of $Fm\bar{3}m$, aligning the S_4 axis with the [001] direction. (b) Mirror plane normals of C_{84} − D_{2d} directed along ⟨100⟩ (c) mirror plane normals directed along ⟨110⟩. The orientation shown in (c) is indicated strongly by Rietveld refinement for the D_{2d} isomer in the isomer pure $K_{8+x}C_{84}$ solid and for both the D_2 and D_{2d} isomers in the mixed isomer phases.

75% of the cube corner sites are occupied, suggesting that these two positions are occupied in a mutually exclusive manner; that is, on 25% of the octahedral sites there are only octahedron center positions occupied and the cube corner positions are empty, whereas on the remaining 75% of the octahedral sites there are complete K_8 cubes without occupancy, and resulting short

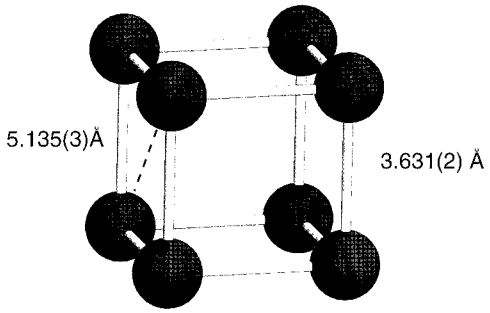

Figure 27. The K_8 cube on the octahedral site of the *fcc* $K_{8+x}C_{84}$ phases.

K−K contacts of the site center. The edge of the K_8 cube is considerably larger than the Na_x units at 3.6 Å, which is consistent with the larger size of potassium (Figure 27). There is no indication from EPR studies of any unpaired spin density on this potassium unit. The phases all appear to be localized electron insulators, although the size of the interanion exchange coupling does appear to vary with the symmetry of the host molecule.

Orientationally ordered phases similar to those in the C_{60} case can therefore be prepared from higher fullerene hosts. Detailed investigation of the structures and electronic properties of a wide range of higher fulleride intercalates, of particular interest at compositions corresponding to half-filling of bands derived from degenerate basis orbitals such as $C_{84}{}^{2-}$—D_{2d}, is now possible.

Conclusion

It is appropriate to return to the question posed initially of whether further study of these extensively investigated materials is worthwhile, as the highest transition temperature of 40 K has not increased in the past two years. A combination of the absence of real predictive power in the solid state and consideration of new theoretical and experimental developments indicates that there are areas of real interest still to be addressed. Recent work shows that key questions remain unanswered, and that these questions link the fullerides to other important areas of solid-state science. The A_3C_{60} compounds are metals despite the interelectron repulsion appearing to be considerably larger than the bandwidth, due to the influence of orbital degeneracy on the Mott−Hubbard model. Magnetic ordering competes with superconductivity, suggesting common features with the copper oxides. Major advances, however, will have to come from breakthroughs in preparative chemistry because the search for higher superconducting transition temperatures now requires the synthesis of new structure types, differing from the simple sphere packings yet retaining electronic contact between the anions. The example of $(NH_3)_8Na_2C_{60}$ shows that these new structures can be constructed using a range of weak intermolecular interactions, and could be effected by borrowing ideas from the fields of supramolecular chemistry and crystal engineering. The higher fullerenes, with different point symmetries and frontier orbital degeneracies, offer an unexplored range of new intercalate structures and unpredictable physical properties.

Acknowledgment. I thank Professor O. Gunnarsson (MPI, Stuttgart), Professor Y. Iwasa (JAIST), and Professor P. W. Fowler (University of Exeter) for discussion. I thank Professor H. Shinohara and Dr. T. J. S. Dennis (Department of Chemistry, Nagoya University) for collaboration in developing the intercalation chemistry of C_{84}, and Dr. S. J. Heyes (Inorganic Chemistry Laboratory, University of Oxford) for his expertise in solid-state NMR spectroscopy. The work referred to in Oxford was carried out with my co-workers K. M. Allen, P. Dahlke, A. C. Duggan, A. J. Fowkes, J. M. Fox, and P. F. Henry, and support from the Leverhulme Trust and the U.K. EPSRC.

References

(1) Haddon, R. C.; Hebard, A. F.; Rosseinsky, M. J.; Murphy, D. W.; Duclos, S. J.; Lyons, K. B.; Miller, B.; Rosamilia, J. M.; Fleming, R. M.; Kortan, A. R.; Glarum, S. H.; Makhija, A. V.; Muller, A. J.; Eick, R. H.; Zahurak, S. M.; Tycko, R.; Dabbagh, G.; Thiel, F. A. *Nature* **1991**, *350*, 320.
(2) Hebard, A. F.; Rosseinsky, M. J.; Haddon, R. C.; Murphy, D. W.; Glarum, S. H.; Palstra, T. T. M.; Ramirez, A. P.; Kortan, A. R. *Nature* **1991**, *350*, 600.
(3) Rosseinsky, M. J. *J. Mater. Chem.* **1995**, *5*, 1497−1513.
(4) Tanigaki, K.; Prassides, K. *J. Mater. Chem.* **1995**, *5*, 1515−1527.
(5) Gunnarsson, O. *Rev. Mod. Phys.* **1997**, *69*, 575−606.
(6) Gelfand, M. P. *Supercond. Rev.* **1994**, *1*, 103.
(7) Ramirez, A. P. *Supercond. Rev.* **1994**, *1*, 1.
(8) Murphy, D. W.; Rosseinsky, M. J.; Fleming, R. M.; Tycko, R.; Ramirez, A. P.; Haddon, R. C.; Siegrist, T.; Dabbagh, G.; Tully, J. C.; Walstedt, R. E. *J. Phys. Chem. Solids* **1992**, *53*, 1321.
(9) Fischer, J. E. *J. Phys. Chem. Solids* **1997**, *58*, 1939.
(10) Prassides, K. *Curr. Opin. Solid State Mater. Sci.* **1997**, *2*, 433.
(11) Kroto, H. W.; Heath, J. R.; O'Brien, S. C.; Curl, R. F.; Smalley, R. E. *Nature* **1985**, *318*, 162.
(12) Kratschmer, W.; Lamb, L. D.; Fostiropoulos, K.; Huffmann, D. R. *Nature* **1990**, *347*, 354.
(13) Tycko, R. *J. Phys. Chem. Solids* **1993**, *54*, 1713−1723.
(14) Chow, P. C.; Jiang, X.; Reiter, G.; Wochner, P.; Moss, S. C.; Axe, J. D.; Hanson, J. C.; McMullan, R. K.; Meng, R. L. *Phys. Rev. Lett.* **1992**, *69*, 2943.
(15) David, W. I. F.; Ibberson, R. M.; Matthewman, J. C.; Prassides, K.; Dennis, T. J. S.; Hare, J. P.; Kroto, H. W.; Taylor, R.; Walton, D. R. M. *Nature* **1991**, *353*, 147.
(16) Tanigaki, K.; Ebbesen, T. W.; Saito, S.; Mizuki, J.; Tsai, J. S.; Kubo, Y.; Kuroshima, S. *Nature* **1991**, *352*, 222.
(17) Prassides, K.; Tomkinson, J.; Christides, C.; Rosseinsky, M. J.; Murphy, D. W.; Haddon, R. C. *Nature* **1991**, *354*, 462.
(18) Duclos, S. J.; Haddon, R. C.; Glarum, S. H.; Hebard, A. F.; Lyons, K. B. *Science* **1991**, *254*, 1625.
(19) Mitch, M. G.; Chase, S. J.; Lannin, J. S. *Phys. Rev. Lett.* **1992**, *68*, 883.
(20) Chen, C.-C.; Lieber, C. M. *J. Am. Chem. Soc.* **1992**, *114*, 3141.
(21) Ramirez, A. P.; Kortan, A. R.; Rosseinsky, M. J.; Duclos, S. J.; Musjce, A. M.; Haddon, R. C.; Murphy, D. W.; Makhija, A. V.; Zahurak, S. M.; Lyons, K. B. *Phys. Rev. Lett.* **1992**, *68*, 1058.
(22) Chakravarty, S.; Kivelson, S. A.; Salkola, M. I.; Tewari, S. *Science* **1992**, *256*, 1306.
(23) Chakravarty, S.; Gelfand, M. P.; Kivelson, S. *Science* **1991**, *254*, 970.
(24) Ramirez, A. P.; Rosseinsky, M. J.; Murphy, D. W.; Haddon, R. C. *Phys. Rev. Lett.* **1992**, *69*, 1687−90.
(25) Quirion, G.; Bourbonnais, C.; Barthel, E.; Auban, P.; Jerome, D.; Lambert, J. M.; Zahab, A.; Bernier, P.; Fabre, C.; Rassat, A. *Europhys. Lett.* **1993**, *21*, 233−238.
(26) Wong, W. H.; Hanson, M. E.; Clark, W. G.; Gruner, G.; Thompson, J. D.; Whetten, R. L.; Huang, S.-M.; Kaner, R. B.; Diederich, F.; Petit, P.; Andre, J.-J.; Holczer, K. *Europhys. Lett.* **1992**, *18*, 79−84.
(27) Palstra, T. T. M.; Hebard, A. F.; Haddon, R. C.; Littlewood, P. B. *Phys. Rev. B* **1994**, *50*, 3462.
(28) Petit, P.; Robert, J.; Yildirim, T.; Fischer, J. E. *Phys. Rev. B* **1996**, *54*, R3764.
(29) Fleming, R. M.; Ramirez, A. P.; Rosseinsky, M. J.; Murphy, D. W.; Haddon, R. C.; Zahurak, S. M.; Makhija, A. V. *Nature* **1991**, *352*, 787−788.
(30) Sparn, G.; Thompson, J. D.; Huang, S.-M.; Kaner, R. B.; Diederich, F.; Whetten, R. L.; Gruner, G.; Holczer, K. *Science* **1991**, *252*, 1829.
(31) Zhou, O.; Vaughan, G. B. M.; Zhu, Q.; Fischer, J. E.; Heiney, P. A.; Coustel, N.; McCauley, J. P.; Smith, A. B. *Science* **1992**, *255*, 833.
(32) Stephens, P. W.; Mihaly, L.; Lee, P. L.; Whetten, R. L.; Huang, S.-M.; Kaner, R.; Diederich, F.; Holczer, K. *Nature* **1991**, *351*, 632−634.

(33) Allen, K. M.; David, W. I. F.; Fox, J. M.; Ibberson, R. M.; Rosseinsky, M. J. *Chem. Mater.* **1995**, *7*, 764−770.
(34) Mazin, I. I.; Lichtenstein, A. I.; Gunnarsson, O.; Andersen, O. K.; Antropov, V. P.; Burkov, S. E. *Phys. Rev. Lett.* **1993**, *70*, 4142.
(35) Teslic, S.; Egami, T.; Fischer, J. E. *Phys. Rev. B* **1995**, *51*, 5973.
(36) Yildirim, T.; Fischer, J. E.; Harris, A. B.; Stephens, P. W.; Liu, D.; Brard, L.; Strongin, R. M.; Smith, A. B. *Phys. Rev. Lett.* **1993**, *71*, 1383−1386.
(37) Kniaz, K.; Fischer, J. E.; Zhu, Q.; Rosseinsky, M. J.; Zhou, O.; Murphy, D. W. *Solid State Commun.* **1993**, *88*, 47.
(38) Prassides, K.; Christides, C.; Thomas, I. M.; Mizuki, J.; Tanigaki, K.; Hirosawa, I.; Ebbesen, T. W. *Science* **1994**, *263*, 950.
(39) Yildirim, T.; Fischer, J. E.; Dinnebier, R.; Stephens, P. W.; Lin, C. L. *Solid State Commun.* **1995**, *93*, 269−274.
(40) Palstra, T. T. M.; Zhou, O.; Iwasa, Y.; Sulewski, P. E.; Fleming, R. M.; Zegarski, B. R. *Solid State Commun.* **1995**, *93*, 327.
(41) Kortan, A. R.; Kopylov, N.; Glarum, S.; Gyorgy, E. M.; Ramirez, A. P.; Fleming, R. M.; Zhou, O.; Thiel, F. A.; Trevor, P. L.; Haddon, R. C. *Nature* **1992**, *360*, 566−568.
(42) Mott, N. F. *Metal−Insulator Transitions*; 2nd ed.; Taylor & Francis: London, 1990.
(43) Gunnarsson, O.; Koch, E.; Martin, R. M. *Phys. Rev. B* **1996**, *54*, R11026.
(44) Lof, R. W.; van Veenendaal, M. A.; Koopmans, B.; Jonkman, H. T.; Sawatzky, G. A. *Phys. Rev. Lett.* **1992**, *68*, 3924.
(45) Bruhwiler, P. A.; Maxwell, A. J.; Nilsson, A.; Martensson, N.; Gunnarsson, O. *Phys. Rev. B* **1992**, *48*, 18296.
(46) Antropov, V. P.; Gunnarsson, O.; Jepsen, O. *Phys. Rev. B* **1992**, *46*, 13647.
(47) Weaver, J. H.; Poirier, D. M. *Solid State Phys.* **1994**, *48*, 1.
(48) Pickett, W. E. *Solid State Phys.* **1994**, *48*, 226.
(49) Duggan, A. C.; Fox, J. M.; Henry, P. F.; Heyes, S. J.; Laurie, D. E.; Rosseinsky, M. J. *Chem. Commun.* **1996**, 1191.
(50) Satpathy, S.; Antropov, V. P.; Andersen, O. K.; Jepsen, O.; Gunnarsson, O.; Lichtenstein, A. I. *Phys. Rev. B* **1992**, *46*, 1773−1793.
(51) Georges, A.; Kotliar, G.; Krauth, W.; Rozenberg, M. J. *Rev. Mod. Phys.* **1996**, *68*, 13.
(52) Gunnarsson, O.; Koch, E.; Martin, R. M. *Phys. Rev. B* **1997**, *56*, 1146.
(53) Aryasetiawan, F.; Gunnarsson, O.; Koch, E.; Martin, R. M. *Phys. Rev. B* **1997**, *55*, R10165.
(54) Auerbach, A.; Manini, N.; Tosatti, E. *Phys. Rev. B* **1994**, *49*, 12998.
(55) Bhyrappa, P.; Paul, P.; Stinchcombe, J.; Boyd, P. D. W.; Reed, C. A. *J. Am. Chem. Soc.* **1993**, *115*, 11004.
(56) Green, W. H.; Gorun, S. M.; Fitzgerald, G.; Fowler, P. W.; Ceulemans, A.; Titeca, B. C. *J. Phys. Chem.* **1996**, *100*, 14892.
(57) Ceulemans, A.; Cibotaru, L. F.; Cimpoesu, F. *Phys. Rev. Lett.* **1997**, *78*, 3725.
(58) Fischer, J. E.; Bendele, G.; Dinnebier, R.; Stephens, P. W.; Lin, C. L.; Bykovetz, N.; Zhu, Q. *J. Phys. Chem. Solids* **1995**, *56*, 1445−1457.
(59) Bendele, G.; Stephens, P. W.; Fischer, J. E. *Europhys. Lett.* **1998**, *41*, 553.
(60) Walstedt, R. E.; Murphy, D. W.; Rosseinsky, M. J. *Nature* **1993**, *362*, 611.
(61) Zimmer, G.; Thier, K.-F.; Mehring, M.; Rachdi, F.; Fischer, J. E. *Phys. Rev. B* **1996**, *53*, 5620.
(62) Gorny, K.; Hahn, C.; Martindale, J. A.; Yu, S.; Pennington, C. H.; Buffinger, D. R.; Ziebarth, R. P. *Phys. Rev. Lett.* **1997**, *79*, 5118.
(63) Yildirim, T.; Barbedette, L.; Fischer, J. E.; Lin, C. L.; Robert, J.; Petit, P.; Palstra, T. T. M. *Phys. Rev. Lett.* **1996**, *77*, 167−170.
(64) Louie, S. G.; Shirley, E. L. *J. Phys. Chem. Solids* **1993**, *54*, 1767.
(65) Fleming, R. M.; Rosseinsky, M. J.; Murphy, D. W.; Ramirez, A. P.; Haddon, R. C.; Siegrist, T.; Tycko, R.; Dabbagh, G.; Hampton, C. *Nature* **1991**, *352*, 701.
(66) Erwin, S. C.; Bruder, C. *Phys. B* **1994**, *199*, 600.
(67) Kiefl, R. F.; Duty, T. L.; Schneider, J. W.; Macfarlane, A.; Chow, K.; Elzey, J. W.; Mendels, P.; Morris, G. D.; Brewer, J. H.; Ansaldo, E. J.; Niedermayer, C.; Noakes, D. R.; Stronach, C. E.; Hitti, B.; Fischer, J. E. *Phys. Rev. Lett.* **1992**, *69*, 2005.
(68) Lukyanchuk, I.; Kirova, N.; Rachdi, F.; Goze, C.; Molinie, P.; Mehring, M. *Phys. Rev. B* **1995**, *51*, 3978.
(69) Kerkoud, R.; Auban-Senzier, P.; Jerome, D.; Lambert, J. M.; Zahab, A.; Bernier, P. *Europhys. Lett.* **1994**, *25*, 379−384.
(70) Kerkoud, R.; Auban-Senzier, P.; Jerome, D.; Brazovskii, S.; Lukyanchuk, I.; Kirova, N.; Rachdi, F.; Goze, C. *J. Phys. Chem. Solids* **1996**, *57*, 143.
(71) Knupfer, M.; Fink, J. *Phys. Rev. Lett.* **1997**, *79*, 2714.
(72) Kuntscher, C. A.; Bendele, G. M.; Stephens, P. W. *Phys. Rev. B* **1997**, *55*, R3366.
(73) Zhou, O.; Cox, D. E. *J. Phys. Chem. Solids* **1992**, *53*, 1373.
(74) Dahlke, P.; Henry, P. F.; Rosseinsky, M. J. *J. Mater. Chem.* **1998**, *8*, 1571.
(75) Prassides, K., personal communication.
(76) Rosseinsky, M. J.; Murphy, D. W.; Fleming, R. M.; Tycko, R.; Ramirez, A. P.; Siegrist, T.; Dabbagh, G.; Barrett, S. E. *Nature* **1992**, *356*, 416−418.
(77) McMillan, W. L. *Phys. Rev.* **1968**, *167*, 331.
(78) Maniwa, Y.; Sugiura, D.; Kume, K.; Kikuchi, K.; Suzuki, S.; Achiba, Y.; Hirosawa, I.; Tanigaki, K.; Shimoda, H.; Iwasa, Y. *Phys. Rev. B* **1996**, *54*, R6861.
(79) Robert, J.; Petit, P.; Yildirim, T.; Fischer, J. E. *Phys. Rev. B* **1998**, *57*, 1226.
(80) Bendele, G. M.; Stephens, P. W.; Prassides, K.; Vavekis, K.; Kordatos, K.; Tanigaki, K. *Phys. Rev. Lett.* **1998**, *80*, 736.
(81) Cristofolini, L.; Kordatos, K.; Lawless, G. A.; Prassides, K.; Tanigaki, K.; Waugh, M. P. *Chem. Commun.* **1997**, 375.
(82) Tanigaki, K.; Hirosawa, I.; Ebbesen, T. W.; Mizuki, J.; Shimakawa, Y.; Kubo, Y.; Kuroshima, S. *Nature* **1992**, *356*, 419.
(83) Diederichs, J.; Schilling, J. S.; Herwig, K. W.; Yelon, W. B. *J. Phys. Chem. Solids* **1997**, *58*, 123.
(84) Burk, B.; Crespi, V. H.; Zettl, A.; Cohen, M. L. *Phys. Rev. Lett.* **1994**, *72*, 3706.
(85) Rodriguez-Martinez, L. M.; Attfield, J. P. *Phys. Rev. B* **1996**, *54*, R15622.
(86) Zhou, O.; Fleming, R. M.; Murphy, D. W.; Rosseinsky, M. J.; van Dover, R. B.; Ramirez, A. P.; Haddon, R. C. *Nature* **1993**, *362*, 433.
(87) Shimoda, H.; Iwasa, Y.; Miyamoto, Y.; Maniwa, Y.; Mitani, T. *Phys. Rev. B* **1996**, *54*, R15653.
(88) Iwasa, Y.; Shimoda, H.; Miyamoto, Y.; Mitani, T.; Maniwa, Y.; Zhou, O.; Palstra, T. T. M. *J. Phys. Chem. Solids* **1997**, *58*, 1697.
(89) Rosseinsky, M. J.; Murphy, D. W.; Fleming, R. M.; Zhou, O. *Nature* **1993**, *364*, 425−427.
(90) Iwasa, Y.; Shimoda, H.; Palstra, T. T. M.; Maniwa, Y.; O.Zhou; T. Mitani *Phys. Rev. B* **1996**, *53*, 8836−8839.
(91) Allen, K. M.; Heyes, S. J.; Rosseinsky, M. J. *J. Mater. Chem.* **1996**, *6*, 1445−1447.
(92) Zhou, O.; Palstra, T. T. M.; Iwasa, Y.; Fleming, R. M.; Hebard, A. F.; Sulewski, P. E. *Phys. Rev. B* **1995**, *52*, 483.
(93) Henry, P. F.; Rosseinsky, M. J.; Watt, C. J. *J. Chem. Soc., Chem. Commun.* **1995**, 2131−2132.
(94) Durand, R.; Fullagar, W. K.; Lindsell, G.; Reynolds, P. A.; White, J. W. *Mol. Phys.* **1995**, *86*, 1.
(95) Fullagar, W. K.; Reynolds, P. A.; White, J. W. *Solid State Commun.* **1997**, *104*, 23.
(96) Allen, K. M.; Henry, P. F.; Millburn, J. E.; Rosseinsky, M. J., unpublished results.
(97) Fowkes, A. J.; Fox, J. M.; Henry, P. F.; Heyes, S. J.; Rosseinsky, M. J. *J. Am. Chem. Soc.* **1997**, *119*, 10413.
(98) Allen, F. H.; Howard, J. A. K.; Hoy, V. J.; Desiraju, G. R.; Reddy, D. S.; Wilson, C. C. *J. Am. Chem. Soc.* **1996**, *118*, 4081−4084.
(99) Hanton, L. R.; Hunter, C. A.; Purvis, D. H. *J. Chem. Soc., Chem. Commun.* **1992**, 1134−1136.
(100) Douthwaite, R. E.; Green, M. A.; Green, M. L. H.; Rosseinsky, M. J. *J. Mater. Chem.* **1996**, *6*, 1913.
(101) Douthwaite, R. E.; Green, M. L. H.; Heyes, S. J.; Rosseinsky, M. J.; Turner, J. F. C. *J. Chem. Soc., Chem. Commun.* **1994**, 1367.
(102) Locke, I. W.; Darwish, A. D.; Kroto, H. W.; Prassides, K.; Taylor, R.; Walton, D. R. M. *Chem. Phys. Lett.* **1994**, *225*, 186.
(103) Yildirim, T.; Zhou, O.; Fischer, J. E.; Bykovetz, N.; Strongin, R. A.; Cichy, M. A.; Smith, A. B.; Lin, C. L.; Jelinek, R. *Nature* **1992**, *360*, 569.
(104) Wertheim, G. K.; Buchanan, D. N. E.; Rowe, J. E. *Chem. Phys. Lett.* **1993**, *202*, 320−324.
(105) Fox, J. M.; Henry, P. F.; Rosseinsky, M. J. *Chem. Commun.* **1996**, 2299.
(106) Oszlanyi, G.; Baumgartner, G.; Faigel, G.; Forro, L. *Phys. Rev. Lett.* **1997**, *78*, 4438.
(107) Kim, J. H.; Petric, A.; Ummat, P. K.; Datars, W. R. *J. Phys. Condens. Matter* **1994**, *6*, 5387.
(108) Mitch, M. G.; Lannin, J. S. *J. Phys. Chem. Solids* **1993**, *54*, 1801.
(109) Armbruster, J. F.; Knupfer, M.; Fink, J. *Z. Phys. B* **1997**, *102*, 55.
(110) Rachdi, F.; Hajji, L.; Galtier, M.; Yildirim, T.; Fischer, J. E.; Goze, C.; Mehring, M. *Phys. Rev. B* **1997**, *56*, 7831.
(111) Andreoni, W.; Giannozzi, P.; Armbruster, J. F.; Knupfer, M.; Fink, J. *Europhys. Lett.* **1996**, *34*, 699.
(112) Andreoni, W.; Giannozzi, P.; Parrinello, M. *Phys. Rev. Lett.* **1994**, *72*, 848−851.
(113) Hajji, L.; Rachdi, F.; Goze, C.; Mehring, M.; Fischer, J. E. *Solid State Commun.* **1996**, *100*, 493.
(114) Iwasa, Y.; Hayashi, H.; Furudate, T.; Mitani, T. *Phys. Rev. B* **1996**, *54*, 14960.
(115) Haddon, R. C.; Brus, L. E.; Raghavachari, K. *Chem. Phys. Lett.* **1986**, *125*, 459.
(116) Fowler, P. W.; Manolopoulos, D. E. *An Atlas of Fullerenes*; Oxford University: New York, 1995.
(117) Nakao, K.; Kurita, N.; Fujita, M. *Phys. Rev. B* **1994**, *49*, 11415.
(118) Knupfer, M.; Poirier, D. M.; Weaver, J. H. *Phys. Rev. B* **1994**, *49*, 8464.

(119) Kobayashi, M.; Akahama, Y.; Kawamura, H.; Shinohara, H.; Sato, H.; Saito, Y. *Phys. Rev. B* **1993**, *48*, 16881.
(120) Lu, J. P.; Gelfand, M. P. *Phys. Rev. B* **1995**, *51*, 16615.
(121) Wang, Z. H.; Dresselhaus, M. S.; Dresselhaus, G.; Wang, K. A.; Eklund, P. C. *Phys. Rev. B* **1994**, *49*, 15890.
(122) Poirier, D. M.; Weaver, J. H.; Kikuchi, K.; Achiba, Y. *Z. Phys. D* **1993**, *26*, 79.
(123) Ito, A.; Akaki, O.; Takahashi, T. *J. Electron Spectrosc. Related Phenom.* **1996**, *78*, 457.
(124) Hino, S.; Matsumoto, K.; Hasegawa, S.; Kamiya, K.; Inokuchi, H.; Morikawa, T.; Takahashi, T.; Seki, K.; Kikuchi, K.; Ikemoto, I.; Achiba, Y. *Chem. Phys. Lett.* **1992**, *190*, 169.
(125) Dennis, T. J. S.; Kai, T.; Tomiyama, T.; Shinohara, H. *Chem-.Commun.* **1998**, 619.
(126) Allen, K. M.; Dennis, T. J. S.; Rosseinsky, M. J.; Shinohara, H. *J. Am. Chem. Soc.* **1998**, *120*, 6681.
(127) Tanigaki, K.; Zhou, O. *J. Phys. 1 France* **1996**, *6*, 2159.
(128) Stephens, P. W.; Bortel, G.; Faigel, G.; Tegze, M.; Janossy, A.; Pekker, S.; Oszlanyi, G.; Forro, L. *Nature* **1994**, *370*, 636.
(129) Prassides, K.; Tanigaki, K.; Iwasa, Y. *Physica C* **1997**, *282−287*, 307.

CM980226P